



# A General Protein O-Glycosylation Gene Cluster Encodes the Species-Specific Glycan of the Oral Pathogen *Tannerella forsythia*: O-Glycan Biosynthesis and Immunological Implications

## OPEN ACCESS

### Edited by:

Catherine Ayn Brissette,  
University of North Dakota,  
United States

### Reviewed by:

Jerry Eichler,  
Ben-Gurion University of the Negev,  
Israel  
Yoann Rombouts,  
UMR5089 Institut de Pharmacologie  
et de Biologie Structurale (IPBS),  
France

### \*Correspondence:

Christina Schäffer  
christina.schaeffer@boku.ac.at

### † Present address:

Markus Windwarder,  
Shire Austria GmbH, Vienna, Austria  
Laura Neumann,  
Boehringer Ingelheim RCV GmbH &  
Co. KG, Vienna, Austria

### Specialty section:

This article was submitted to  
Microbial Physiology and Metabolism,  
a section of the journal  
Frontiers in Microbiology

**Received:** 08 May 2018

**Accepted:** 09 August 2018

**Published:** 28 August 2018

### Citation:

Tomek MB, Maresch D,  
Windwarder M, Friedrich V,  
Janesch B, Fuchs K, Neumann L,  
Nimeth I, Zwickl NF, Dohm JC,  
Everest-Dass A, Kolarich D,  
Himmelbauer H, Altmann F and  
Schäffer C (2018) A General Protein  
O-Glycosylation Gene Cluster  
Encodes the Species-Specific Glycan  
of the Oral Pathogen *Tannerella  
forsythia*: O-Glycan Biosynthesis  
and Immunological Implications.  
*Front. Microbiol.* 9:2008.  
doi: 10.3389/fmicb.2018.02008

Markus B. Tomek<sup>1</sup>, Daniel Maresch<sup>2</sup>, Markus Windwarder<sup>2†</sup>, Valentin Friedrich<sup>1</sup>, Bettina Janesch<sup>1</sup>, Kristina Fuchs<sup>1</sup>, Laura Neumann<sup>2†</sup>, Irene Nimeth<sup>1</sup>, Nikolaus F. Zwickl<sup>3</sup>, Juliane C. Dohm<sup>3</sup>, Arun Everest-Dass<sup>4</sup>, Daniel Kolarich<sup>4</sup>, Heinz Himmelbauer<sup>3</sup>, Friedrich Altmann<sup>2</sup> and Christina Schäffer<sup>1\*</sup>

<sup>1</sup> NanoGlycobiology Unit, Department of NanoBiotechnology, Universität für Bodenkultur Wien, Vienna, Austria, <sup>2</sup> Division of Biochemistry, Department of Chemistry, Universität für Bodenkultur Wien, Vienna, Austria, <sup>3</sup> Bioinformatics Group, Department of Biotechnology, Universität für Bodenkultur Wien, Vienna, Austria, <sup>4</sup> Institute for Glycomics, Griffith University, Brisbane, QLD, Australia

The cell surface of the oral pathogen *Tannerella forsythia* is heavily glycosylated with a unique, complex deca-saccharide that is O-glycosidically linked to the bacterium's abundant surface (S-) layer, as well as other proteins. The S-layer glycoproteins are virulence factors of *T. forsythia* and there is evidence that protein O-glycosylation underpins the bacterium's pathogenicity. To elucidate the protein O-glycosylation pathway, genes suspected of encoding pathway components were first identified in the genome sequence of the ATCC 43037 type strain, revealing a 27-kb gene cluster that was shown to be polycistronic. Using a gene deletion approach targeted at predicted glycosyltransferases (Gtfs) and methyltransferases encoded in this gene cluster, in combination with mass spectrometry of the protein-released O-glycans, we show that the gene cluster encodes the species-specific part of the *T. forsythia* ATCC 43037 deca-saccharide and that this is assembled step-wise on a pentasaccharide core. The core was previously proposed to be conserved within the *Bacteroidetes* phylum, to which *T. forsythia* is affiliated, and its biosynthesis is encoded elsewhere on the bacterial genome. Next, to assess the prevalence of protein O-glycosylation among *Tannerella* sp., the publicly available genome sequences of six *T. forsythia* strains were compared, revealing gene clusters of similar size and organization as found in the ATCC 43037 type strain. The corresponding region in the genome of a periodontal health-associated *Tannerella* isolate showed a different gene composition lacking most of the genes commonly found in the pathogenic strains. Finally, we investigated whether differential cell surface glycosylation impacts *T. forsythia*'s overall immunogenicity. Release of proinflammatory cytokines by dendritic cells (DCs) upon stimulation with defined Gtf-deficient mutants of the type strain was measured and their T cell-priming potential

post-stimulation was explored. This revealed that the O-glycan is pivotal to modulating DC effector functions, with the *T. forsythia*-specific glycan portion suppressing and the pentasaccharide core activating a Th17 response. We conclude that complex protein O-glycosylation is a hallmark of pathogenic *T. forsythia* strains and propose it as a valuable target for the design of novel antimicrobials against periodontitis.

**Keywords:** carbohydrate-active enzymes, glycosyltransferase, immunogenicity, locus for glycosylation, methyltransferase, periodontitis, S-layer

## INTRODUCTION

Protein glycosylation in bacteria is a frequent modification of secreted and cell-surface proteins, such as flagella, pili, autotransporters, and surface (S-) layer proteins (Upreti et al., 2003; Schäffer and Messner, 2017). The biological roles of these glycoproteins strongly depend on the bacteria's environmental context and cannot be predicted *a priori* (Varki et al., 2017). In several cases, general protein glycosylation systems are employed, yielding a suite of proteins with diverse locations and functionalities that carry one or more copies of an identical glycan (Schäffer and Messner, 2017). In bacterial genomes, the genetic information governing protein glycosylation is frequently organized in protein glycosylation gene clusters (Nothaft and Szymanski, 2010), which encode nucleotide sugar pathways genes, genes for Gtfs, glycan processing and modifying enzymes, ligases, and transporters. Based on our current knowledge, in bacteria, O-linked protein glycosylation (where the glycan is linked to Ser, Thr, or Tyr residues of the protein) seems to be more prevalent than N-linked protein glycosylation (where the glycan is bound to Asn) (Schäffer and Messner, 2017). Most protein O-glycosylation systems investigated so far secrete virulence factors or translocate glycoproteins to the bacterial cell surface, exemplified with *Campylobacter* spp. (Szymanski et al., 1999, 2003), *Neisseria* spp. (Ku et al., 2009; Vik et al., 2009; Hartley et al., 2011), *Bacteroides* spp. (Fletcher et al., 2009), *Actinomycetes* (Espitia et al., 2010), *Francisella tularensis* (Egge-Jacobsen et al., 2011), *Acinetobacter* spp. (Iwashkiw et al., 2012; Lees-Miller et al., 2013; Harding et al., 2015), *Burkholderia*

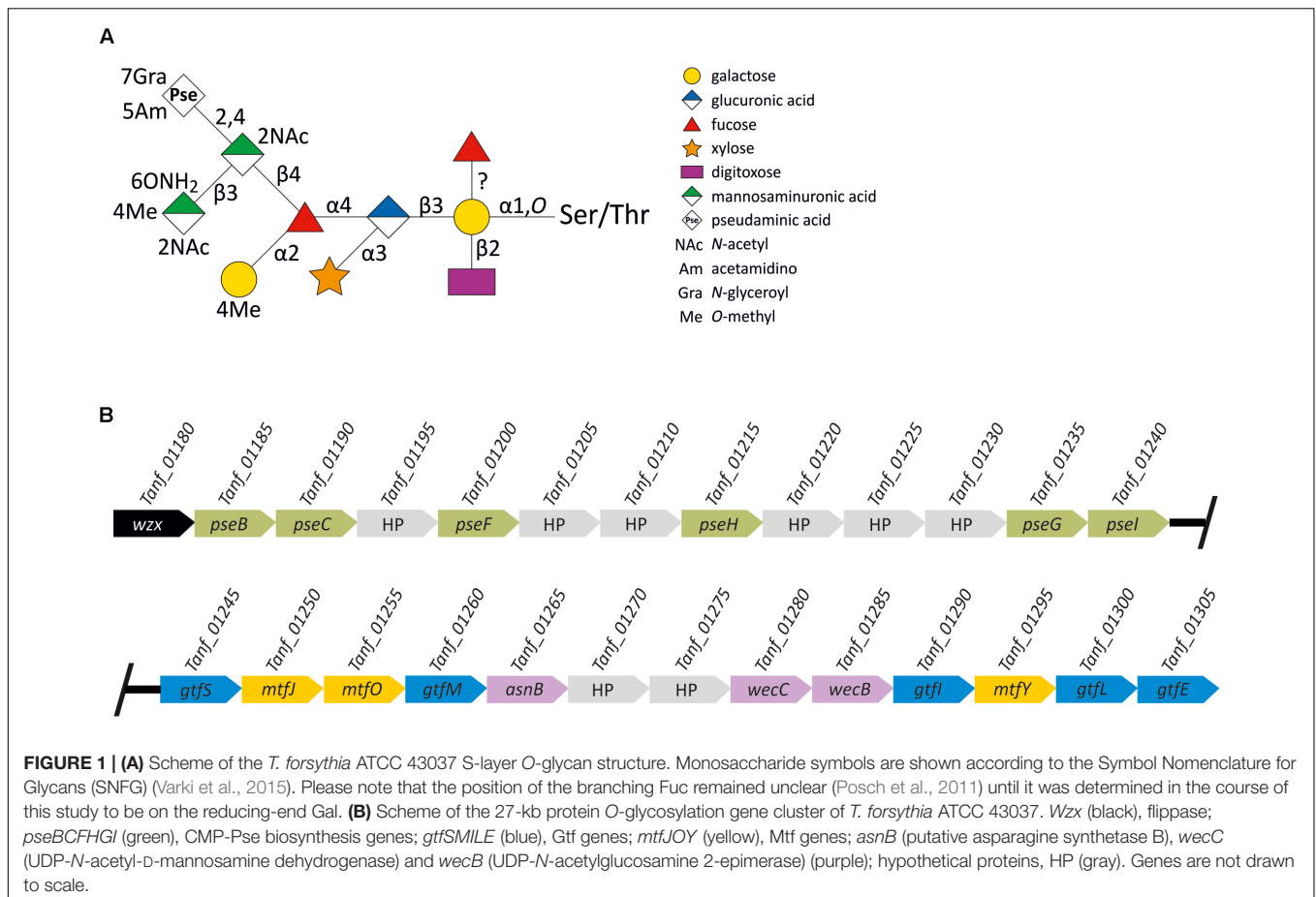
*cepacia* (Lithgow et al., 2014), *Ralstonia solanacearum* (Elhenawy et al., 2016), and *Tannerella forsythia* (Posch et al., 2011).

*Tannerella forsythia* is a Gram-negative pathogen affiliated to the *Bacteroidetes* phylum of bacteria which utilizes a general protein O-glycosylation system to decorate several of its proteins with a so far unique, complex deca-saccharide. The most abundant cellular proteins targeted by this system are the S-layer proteins TfsA and TfsB, which self-assemble on the bacterium's cell surface into a two-dimensional crystalline monolayer (Sekot et al., 2012). The *T. forsythia* O-glycan (**Figure 1A**) is bound to distinct Ser and Thr residues within the three-amino acid motif D(S/T)(A/I/L/M/T/V) (Posch et al., 2011). The glycan is strain-specifically decorated with a modified terminal nonulosonic acid, which can be either a Pse as shown for the ATCC 43037 type strain, or a Leg exemplified by strain UB4 (Friedrich et al., 2017). Besides these sialic acid mimics, other unique S-layer glycan sugars present in the *T. forsythia* O-glycan are  $\alpha$ -L-fucose (Fuc), Dig, Xyl, N-acetyl mannosaminuronic acid (ManNAcA), and N-acetyl mannosaminuronamide (ManNAcCONH<sub>2</sub>) (Posch et al., 2011).

To investigate the biosynthesis of the *T. forsythia* O-glycan, in a previous study, parts of an S-layer protein O-glycosylation gene locus were identified in the *T. forsythia* ATCC 43037 genome, and clustering of highly homologous genes was observed in different *Bacteroidetes* species (Posch et al., 2011). Based on that and a successful protein cross-glycosylation experiment between *T. forsythia* and *Bacteroides fragilis* (Posch et al., 2013), which both belong to the *Bacteroidetes* phylum, the presence of a phylum-wide protein O-glycosylation system was proposed (Coyne et al., 2013). An antiserum raised to a defined, truncated glycan of *B. fragilis* reacted with all *Bacteroidetes* species tested, including *T. forsythia*, but not with the full glycan, suggesting a discrimination between a core glycan and a species-specific glycan portion (Coyne et al., 2013).

In its native environment, *T. forsythia* thrives in a polymicrobial biofilm community that constitutes what is clinically described as oral plaque (Socransky et al., 1998; Holt and Ebersole, 2005). *Tannerella forsythia* is recognized as a key periodontal pathogen following the polymicrobial synergy and dysbiosis model of periodontal disease etiology (Hajishengallis and Lamont, 2012; Lamont and Hajishengallis, 2015). In this model, low abundance keystone pathogens are crucial as they initially subvert host immune responses, further leading to homeostasis breakdown in the oral cavity and destructive inflammation. Recent studies provided evidence that *T. forsythia* employs its unique cell surface to colonize its niche within the polymicrobial biofilm and to orchestrate the immune response

**Abbreviations:** Ac, N-acetyl or acetamido; Am, N-acetimidoyl or acetamidino; APC, antigen presenting cell; BHI, brain heart infusion; BMDC, bone marrow-derived dendritic cell; Cat, chloramphenicol; cDNA, copy DNA; CFSE, carboxyfluorescein succinimidyl ester; CMP, cytidine-5'-monophosphate; Dig, digitoxose; DC, dendritic cell; DMEM, Dulbecco's Modified Eagle's Medium; Erm, erythromycin; ESI, electrospray ionization; Fuc, fucose; Gal, galactose; Gc, N-glycolyl; GDP, guanosine-5'-diphosphate; GM-CSF, granulocyte-macrophage colony-stimulating factor; Gra, N-glyceroyl or N-2,3-dihydroxypropionyl or glycerate group; Gtf, glycosyltransferase; IL, interleukin; INF, interferon; LB, lysogeny broth; LC, liquid chromatography; Leg, legionaminic acid (Leg5,7Ac<sub>2</sub>), 5,7-diacetamido-3,5,7,9-tetra-deoxy-D-glycero-D-galacto-nonulosonic acid; LFG, locus for glycosylation; LPS, lipopolysaccharide; MHC, major histocompatibility complex; Mtf, methyltransferase; MS, mass spectrometry; OP, Octaplas medium; ORF, open reading frame; OTase, oligosaccharyltransferase; PBMC, peripheral blood mononuclear cell; PGC, porous graphitized carbon; PRR, pattern recognition receptor; Pse, pseudaminic acid (Pse5,7Ac<sub>2</sub>), 5,7-diacetamido-3,5,7,9-tetra-deoxy-L-glycero-L-manno-nonulosonic acid; SAM, S-adenosyl-L-methionine; SDS-PAGE, sodium dodecyl sulfate-polyacrylamide gel electrophoresis; Th, T helper cell; TNF, tumor necrosis factor; Tregs, regulatory T cells; UDP, uridine-5'-diphosphate; und-PP, undecaprenyl pyrophosphate; Xyl, xylose.



of resident host tissue and the immune system (Bloch et al., 2017, 2018). In fact, the two S-layer glycoproteins (Sabet et al., 2003; Sharma, 2010; Sekot et al., 2011), as well as a leucine-rich repeat outer membrane glycoprotein BspA (Sharma et al., 2005), are among the bacterium's virulence factors. The S-layer is strongly antigenic and mediates hemagglutination, as well as adherence to and invasion of human gingival epithelial cells (Sabet et al., 2003; Lee et al., 2006; Sakakibara et al., 2007). Studies with human macrophages and gingival fibroblasts demonstrated that the S-layer attenuates the host immune response by evading recognition by the innate immune system, at least at the early stage of infection (Sekot et al., 2011). There are indications that specifically the S-layer O-glycan is crucial for the modulation of host immunity through Th17 suppression (Settem et al., 2013). A very recent study suggests a role specifically of the modified Pse residue (Pse5Am7Gra) present at terminal position on the *T. forsythia* ATCC 43037 O-glycan in facilitating immune evasion by dampening the response of epithelial tissues to initial infection (Bloch et al., 2018). In addition to its immunological relevance, it was shown that the glycosylated *T. forsythia* S-layer plays a role in the bacterium's biofilm life-style (Honma et al., 2007; Bloch et al., 2017; Friedrich et al., 2017).

These data indicate that the *T. forsythia* O-glycan and, hence, its biosynthesis pathway could be valuable targets in efforts to interfere with the establishment of periodontitis, which continues

to be the most frequent inflammatory disease of bacterial origin world-wide (Hajishengallis, 2015). Thus, this present study was designed to obtain insight into the *T. forsythia* O-glycoprotein biosynthesis pathway and its involvement in underpinning the bacterium's pathogenicity. Specifically, emphasis was focused on (i) sequence comparison of the general protein O-glycosylation gene cluster of the *T. forsythia* ATCC 43037 type strain with what is found in other *T. forsythia* strains for which genome sequences were available in public databases; (ii) transcriptional analysis of the protein O-glycosylation gene cluster of *T. forsythia* ATCC 43037; (iii) construction of defined *T. forsythia* mutants deficient in predicted Gtfs and Mtfs encoded in the gene cluster and subsequent analysis of the O-glycans by MS to delineate the roles of the individual enzymes in glycan biosynthesis; and (iv) dissecting an O-glycan structure–function relationship in the immune response of DCs upon stimulation with the *T. forsythia* wild-type versus defined glycosylation-deficient mutants.

## MATERIALS AND METHODS

### Bacterial Strains and Cultivation Conditions

*Tannerella forsythia* ATCC 43037 (American Type Culture Collection – ATCC, Manassas, VA, United States)

(Tanner et al., 1986; Friedrich et al., 2015) and its mutants (**Table 1**) were grown anaerobically in brain heart infusion (BHI) media (Oxoid, Basingstoke, United Kingdom), supplemented with yeast extract (Sigma-Aldrich, Vienna, Austria), L-cysteine (Sigma-Aldrich), hemin (Sigma-Aldrich), menadione (Sigma-Aldrich), N-acetylmuramic acid (Carbosynth, Compton, United Kingdom), and horse serum (Thermo Fisher Scientific, Vienna, Austria) as described previously (Tomek et al., 2017). Media were supplemented with 50 µg/ml gentamicin, 5 µg/ml Erm or 10 µg/ml Cat, when appropriate.

*Escherichia coli* strains (**Table 1**) were grown under standard conditions in LB medium supplemented with 100 µg/ml ampicillin, when appropriate.

## Identification of a Protein O-Glycosylation Gene Cluster in *T. forsythia*

Up- and downstream regions of the previously identified protein O-glycosylation gene locus (Posch et al., 2011) were bioinformatically inspected using the genome sequence of the *T. forsythia* ATCC 43037 type strain as a basis (Friedrich et al., 2015). Information on putative gene functions were obtained through homology searches using the NCBI BLAST suite<sup>1</sup> (Altschul et al., 1997) and the PFAM database<sup>2</sup> (Finn et al., 2016).

An alignment of protein O-glycosylation gene clusters from different *T. forsythia* strains for which genome sequences were publically available was generated using the software MultiGeneBlast 1.1.13 (Camacho et al., 2009; Medema et al., 2013) in “homology search” mode. Genomes and annotations included in the analysis are listed in **Supplementary Table S1**. The genome assembly from *T. forsythia* FDC 92A2 was used as query, restricted to the genomic region from coordinates 1,135,922 to 1,166,078. The database was built from the assemblies of strains ATCC 43037, KS16, 3313, UB4, UB20, UB22 and *Tannerella* sp. HOT-286 (phylo type BU063). The assemblies were downloaded as GenBank flat files (gbff) from the NCBI ftp server<sup>3</sup>. RefSeq assemblies were downloaded for genomes FDC 92A2, ATCC 43037, KS16, 3313 and BU063. For strains UB4, UB20, and UB22, GenBank assemblies containing annotations generated in the context of the initial characterization of these genomes were used (Stafford et al., 2016). The RefSeq gbff files had to be adapted in order to provide unique protein identifiers in regions of interest as input for MultiGeneBlast. Minimal sequence identity (-minperc) and minimal sequence coverage (-minseqcov) for protein alignments were both set to 50%, and default parameters -syntenyweight 0.5, -distancekb 20, -hitspergene 250 were used. For generating the BU063 track, an additional run with lower thresholds, i.e., 10% sequence identity and 10% sequence coverage, was performed. MultiGeneBlast runs were carried out under Linux Ubuntu 16.04; Linux shell commands were used for editing input files. The graphic files generated by MultiGeneBlast were combined and edited.

<sup>1</sup> <https://blast.ncbi.nlm.nih.gov>

<sup>2</sup> <http://pfam.xfam.org>

<sup>3</sup> <ftp://ftp.ncbi.nlm.nih.gov/genomes>

## RNA Purification and Reverse Transcription-PCR

Total RNA was extracted from *T. forsythia* ATCC 43037 using the PureLink RNA Mini Kit (Thermo Fisher Scientific) and subsequently treated with RNase-free DNase (PureLink DNase Set, Thermo Fisher Scientific) to remove DNA contamination. cDNA was generated using the MultiScribe Reverse Transcriptase from the High-Capacity cDNA Reverse Transcription Kit (Thermo Fisher Scientific) using 500 ng of total RNA. One tenth of each cDNA reaction mixture was used as template for PCR using Phusion High-Fidelity DNA polymerase (Thermo Fisher Scientific). The synthesized cDNA was amplified by PCR with primer pairs spanning stepwise neighboring genes, starting at the 5' end of the gene cluster with *Tanf\_01180-Tanf\_01185* and ending with *Tanf\_01300-Tanf\_01305* (**Supplementary Figure S1**). Primer pairs and the size of the corresponding transcripts are indicated for each transcript in **Supplementary Figure S1** and primer sequences are listed in **Supplementary Table S2**. As a positive control, genomic DNA was used, and DNase treated RNA without the cDNA-generating step served as a control for contamination of total RNA with chromosomal DNA.

## Construction of Glycosyltransferase- and Methyltransferase-Deficient Mutants

Four putative Gtf genes (*Tanf\_01260*; *Tanf\_01290*; *Tanf\_01300*; *Tanf\_01305*) and three putative Mtf genes (*Tanf\_01250*; *Tanf\_01255*; *Tanf\_01295*) encoded in the *T. forsythia* ATCC 43037 genome were individually knocked-out by homologous recombination, using a knock-out cassette deleting the selected gene. Clones viable on Erm-containing BHI-agar plates (0.8% w/v) were selected and further tested by PCR for correct integration of the knock-out cassette (**Supplementary Figures S2–S8**). A detailed description of the construction of the knock-out cassettes is given in the **Supplementary Material**. In short, approximately 1-kbp up- and downstream homology regions were joined to the Erm-resistance gene (*PermF*, 1093-bp; *ermF*, 805-bp) by overlap-extension (OE)-PCR and subsequently blunt-end cloned into the plasmid pJET1.2 (Thermo Fisher Scientific). Knock-out cassettes were transformed into electrocompetent *T. forsythia* cells, which were regenerated overnight and plated on Erm-containing BHI selection plates. Single colonies were picked and used for inoculation of BHI medium. Once bacterial growth was visible, genomic DNA was isolated (Cheng and Jiang, 2006) and the loss of the selected gene (log) was tested by PCR (**Supplementary Figures S2–S8**). Phusion High-Fidelity DNA polymerase (Thermo Fisher Scientific) or Herculase II Fusion DNA Polymerase (Agilent Technologies, Vienna, Austria) were used for PCR amplification according to the manufacturer's instructions. Oligonucleotides (Thermo Fisher Scientific) used are listed in **Supplementary Tables S3, S4**.

To exclude possible polar effects leading to an altered transcription of downstream genes, Gtf-deficient mutants were complemented with the native gene, in combination with a Cat resistance gene (chloramphenicol acetyl transferase, *cat*;



**TABLE 1** | Bacterial strains and plasmids used in this study.

Strain or plasmid	Genotype and use or description	Source or reference
<b>Escherichia coli strain</b>		
DH5 $\alpha$	F <sup>-</sup> $\Phi$ 80lacZ $\Delta$ M15 $\Delta$ (lacZYA-argF) U169 recA1 endA1 hsdR17 (rK <sup>-</sup> , mK <sup>+</sup> ) phoA supE44 $\lambda$ -thi-1 gyrA96 relA1; cloning strain	Invitrogen, Austria
<b>Tannerella forsythia strains</b>		
ATCC 43037	Type strain, wild-type	ATCC; Friedrich et al., 2015
ATCC 43037 $\Delta$ Tanf_01245	$\Delta$ Tanf_01245::ermF; knock-out strain of Tanf_01245	Tomek et al., 2017
ATCC 43037 $\Delta$ Tanf_01245 <sup>+</sup>	$\Delta$ Tanf_01245::Tanf_01245 cat; reconstituted knock-out strain	Tomek et al., 2017
ATCC 43037 $\Delta$ Tanf_01250	$\Delta$ Tanf_01250::ermF; knock-out strain of Tanf_01250	This work
ATCC 43037 $\Delta$ Tanf_01255	$\Delta$ Tanf_01255::ermF; knock-out strain of Tanf_01255	This work
ATCC 43037 $\Delta$ Tanf_01260	$\Delta$ Tanf_01260::ermF; knock-out strain of Tanf_01260	This work
ATCC 43037 $\Delta$ Tanf_01260 <sup>+</sup>	$\Delta$ Tanf_01260::Tanf_01260 cat; reconstituted knock-out strain	This work
ATCC 43037 $\Delta$ Tanf_01290	$\Delta$ Tanf_01290::ermF; knock-out strain of Tanf_01290	This work
ATCC 43037 $\Delta$ Tanf_01290 <sup>+</sup>	$\Delta$ Tanf_01290::Tanf_01290 cat; reconstituted knock-out strain	This work
ATCC 43037 $\Delta$ Tanf_01295	$\Delta$ Tanf_01295::ermF; knock-out strain of Tanf_01295	This work
ATCC 43037 $\Delta$ Tanf_01300	$\Delta$ Tanf_01300::ermF; knock-out strain of Tanf_01300	This work
ATCC 43037 $\Delta$ Tanf_01300 <sup>+</sup>	$\Delta$ Tanf_01300::Tanf_01300 cat; reconstituted knock-out strain	This work
ATCC 43037 $\Delta$ Tanf_01305	$\Delta$ Tanf_01305::(Perm)-ermF; knock-out strain of Tanf_01305	This work
ATCC 43037 $\Delta$ Tanf_01305 <sup>+</sup>	$\Delta$ Tanf_01305::Tanf_01305 cat; reconstituted knock-out strain	This work
<b>Plasmids</b>		
pJET1.2/blunt	Cloning vector; amp <sup>R</sup>	Thermo Fisher Scientific
pJET/ $\Delta$ TF0955ko	Vector for amplification of the erythromycin resistance gene	Tomek et al., 2014
pEXALV	Vector for amplification of the chloramphenicol resistance gene	Zarschler et al., 2009
pJET1.2/ $\Delta$ Tanf_01250	Tanf_01250 knock-out cassette; amp <sup>R</sup> ermF <sup>R</sup>	This work
pJET1.2/ $\Delta$ Tanf_01250 <sup>+</sup>	Cassette for reconstitution of $\Delta$ Tanf_01250; amp <sup>R</sup> cat <sup>R</sup>	This work
pJET1.2/ $\Delta$ Tanf_01255	Tanf_01255 knock-out cassette; amp <sup>R</sup> ermF <sup>R</sup>	This work
pJET1.2/ $\Delta$ Tanf_01260	Tanf_01260 knock-out cassette; amp <sup>R</sup> ermF <sup>R</sup>	This work
pJET1.2/ $\Delta$ Tanf_01260 <sup>+</sup>	Cassette for reconstitution of $\Delta$ Tanf_01260; amp <sup>R</sup> cat <sup>R</sup>	This work
pJET1.2/ $\Delta$ Tanf_01290	Tanf_01290 knock-out cassette; amp <sup>R</sup> ermF <sup>R</sup>	This work
pJET1.2/ $\Delta$ Tanf_01290 <sup>+</sup>	Cassette for reconstitution of $\Delta$ Tanf_01290; amp <sup>R</sup> cat <sup>R</sup>	This work
pJET1.2/ $\Delta$ Tanf_01295	Tanf_01295 knock-out cassette; amp <sup>R</sup> ermF <sup>R</sup>	This work
pJET1.2/ $\Delta$ Tanf_01300	Tanf_01300 knock-out cassette; amp <sup>R</sup> ermF <sup>R</sup>	This work
pJET1.2/ $\Delta$ Tanf_01300 <sup>+</sup>	Cassette for reconstitution of $\Delta$ Tanf_01300; amp <sup>R</sup> cat <sup>R</sup>	This work
pJET1.2/ $\Delta$ Tanf_01305	Tanf_01305 knock-out cassette; amp <sup>R</sup> ermF <sup>R</sup>	This work
pJET1.2/ $\Delta$ Tanf_01305 <sup>+</sup>	Cassette for reconstitution of $\Delta$ Tanf_01305; amp <sup>R</sup> cat <sup>R</sup>	This work

650 bp) for selection. For this purpose, the approximately 1-kbp homologous upstream region plus the associated native Gtf gene were joined to the *cat* resistance gene using OE-PCR and subsequently blunt-end cloned into the plasmid pJET1.2. Using the artificially introduced restriction sites SphI and KpnI, the approximately 1-kbp downstream homologous region was added, completing the reconstitution cassettes for *Tanf\_01260* and *Tanf\_01290* (Supplementary Figures S2, S3). The downstream region of the *Tanf\_01300* reconstitution cassette was cloned via KpnI and NdeI restriction sites, while KpnI and BamHI were used for the *Tanf\_01305* reconstitution cassette (Supplementary Figures S4, S5).

## SDS-PAGE and Western-Blotting

SDS-PAGE of crude cell extracts was carried out according to Laemmli (1970). 7.5% SDS-PA gels were prepared according to a standard protocol. Proteins were visualized with colloidal Coomassie Brilliant Blue (CBB) R-250 (Serva, Heidelberg,

Germany) or transferred onto a polyvinylidene difluoride (PVDF) membrane (Bio-Rad, Vienna, Austria) for Western-blot analysis. Polyclonal rabbit antisera raised against the recombinant S-layer proteins TfsA ( $\alpha$ -TfsA) and TfsB ( $\alpha$ -TfsB) (Sekot et al., 2012) were used as primary antibodies in combination with a monoclonal goat  $\alpha$ -rabbit secondary antibody labeled with IRDye 800CW (LI-COR Biosciences, Lincoln, NE, United States). S-Layer protein bands were visualized at 800 nm using an Odyssey Infrared Imaging System (LI-COR Biosciences).

## S-Layer O-Glycan Preparation and Liquid Chromatography ESI-MS

O-Glycans were released from the glycosylated S-layer proteins TfsA and TfsB by in-gel reductive  $\beta$ -elimination and purified by preparative PGC-HPLC as described previously (Posch et al., 2011; Tomek et al., 2014). The glycan mixture was analyzed using a Dionex Ultimate 3000 system directly linked to an

ion trap instrument (amaZon speed ETD, Bruker, Germany) equipped with the standard ESI source in positive ion, Data Dependent Acquisition (DAA) mode (performing MS/MS on signals based on their intensity and LC elution). MS-scans were recorded over an  $m/z$  range 450–1650; ICC target was set to 100,000 and maximum accumulation time to 200 ms. The top 10 highest peaks were selected for fragmentation with an absolute intensity threshold above 50,000. Instrument calibration was performed using ESI Tuning Mix (Agilent Technologies) as by the manufacturer's recommendations. LC separation of released O-glycans was performed on a Thermo Hypercarb separation column (5  $\mu\text{m}$  particle size; 100 mm  $\times$  0.360 mm). A gradient from 1 to 21% solvent B in solvent A (solvent A, 65 mM ammonium formate buffer, pH 3.0; solvent B, 100% acetonitrile) over 20 min was applied, followed by a 10-min gradient from 21% B to 50% B, at a flow rate of 6  $\mu\text{l}/\text{min}$ . Data were evaluated manually using the DataAnalysis 4.0 software (Bruker) and Glycoworkbench 2.1 build 146 (Ceroni et al., 2008).

## Generation of Human Monocyte- and Murine Bone Marrow-Derived Dendritic Cells

Human monocytes (E59;  $\sim 40 \times 10^6$  cells) from healthy volunteers (Ethical approval EK 1880/2012 in accordance with the Declaration of Helsinki, Medical University of Vienna, Vienna, Austria; written informed consent was obtained from all volunteers of this study) were thawed at 37°C and placed into AIM V medium (Gibco, Life Technologies, Paisley, United Kingdom) supplemented with 2% human plasma (Octaplas, OP; Octapharma, Zurich, Switzerland). Monocytes were counted and adjusted to a concentration of  $0.5 \times 10^6$  cells/ml. Dead cells were removed after incubation at 37°C for 1.5 h, while living cells were differentiated with 1000 U/ml GM-CSF and 400 U/ml IL-4. Medium including cytokines was replaced on day 3 and iDCs were harvested on day 5 (Lanzinger et al., 2012).

Murine BMDCs were isolated from C57BL/6 mice (Gallucci et al., 1999). Briefly, femurs and tibias were rinsed with DMEM, supplemented with 10% heat-inactivated fetal calf serum (FCS; PAA, Pasching Austria), 1% penicillin/streptomycin (Gibco), 1% non-essential amino acids (NEAA) (Gibco) and 0.0002%  $\beta$ -mercaptoethanol (Sigma-Aldrich). Erythrocytes were lysed in erytholysis buffer (0.15 M  $\text{NH}_4\text{Cl}$ , 10 mM  $\text{KHCO}_3$ , 0.1 mM  $\text{Na}_2\text{EDTA}$ ; pH 7.2). The bone marrow was washed, and cells were re-suspended in supplemented DMEM. Cells were cultured in 24-well plates (Iwaki, Japan) at a concentration of  $1.0 \times 10^6$  cells per well in DMEM supplemented with 10% FCS and in the presence of 5 ng/ml recombinant murine IL-4 (eBioscience, San Diego, CA, United States) and 3 ng/ml recombinant murine GM-CSF (BD Pharmingen, San Diego, CA, United States). Half of the medium (including all supplements) was replaced every second day. Immature DCs (iDs) were harvested on day 6, counted and adjusted to a concentration of  $1.0 \times 10^6$  cells/ml. All mouse experiments were performed in accordance with the institutional guidelines and approved by the Animal Care and Use Committee of the Medical University of Vienna, Austria (GZ: 856861/2013/16).

## Stimulation of Dendritic Cells With Inactivated T. forsythia Cells

*Tannerella forsythia* wild-type and Gtf-deficient mutants were irradiated three times with UV light using maximum UV energy settings for 1 min, each, (Ultraviolet Crosslinker CL-1000; UVP, Upland, CA, United States) for inactivation. Cell integrity after treatment was verified by scanning electron microscopy using an Inspect S50 scanning electron microscope (FEI, Eindhoven, Netherlands) (Tomek et al., 2014).

Murine and human iDCs were matured in a 48-well plate with inactivated *T. forsythia* wild-type,  $\Delta\text{Tanf}_{01245}$  ( $\Delta\text{gtfS}$ ),  $\Delta\text{Tanf}_{01290}$  ( $\Delta\text{gtfI}$ ), or  $\Delta\text{Tanf}_{01305}$  ( $\Delta\text{gtfE}$ ) cells, at concentrations of  $10^6$ ,  $10^7$  and  $10^8$  cfu/ml. iDCs stimulated with 100 ng/ml LPS (*E. coli* strain O111:B4, Calbiochem, EMD Chemicals, San Diego, CA, United States) served as a positive control. Stimulated DCs were incubated at 37°C for 24 h. Supernatants were frozen for later use, DCs were harvested. DC maturation was monitored by visual and flow cytometric evaluation of typical DC morphology (LSR II flow cytometer, BD Biosciences), and expression of cell-surface markers ( $\alpha$ -CD80,  $\alpha$ -CD86,  $\alpha$ -MHC-II; eBioscience) after 6 h and 24 h, respectively.

## Determination of Cytokine Levels by ProcartaPlex Multiplex Immunoassay and ELISA

Multiplex cytokine analysis of human monocyte-derived DC supernatants was performed using ProcartaPlex Multiplex immunoassay (eBioscience) for measuring cytokine secretion of IFN- $\gamma$ , IL-1 $\alpha$ , IL-1 $\beta$ , IL-4, IL-6, IL-10, IL-12p70, IL-23, and TNF- $\alpha$ .

The level of secreted cytokines in murine BMDC supernatants, TNF- $\alpha$  and IL-6, were analyzed using commercial ready-set-go ELISA kits (eBioscience) in 96-well microtiter plates according to the manufacturer's protocol and measured at 450 nm by a micro plate reader (PerkinElmer, EnSpire Multimode Reader, Waltham, MA, United States).

## T Cell-Priming Upon Stimulation of Antigen-Presenting Cells With T. forsythia

Human PBMCs were separated from whole blood by density centrifugation (Lanzinger et al., 2012). PBMCs were cultured in RPMI-1640 medium supplemented with GlutaMAX-I (Gibco) and 2% human plasma (OP, Octapharma). PBMCs were counted with BD Trucount tubes (BD Biosciences), adjusted to a concentration of  $1.0 \times 10^7$  cells/ml and labeled with CFSE (Invitrogen, Austria). T cell priming upon antigen-presenting cell (APC) stimulation with *T. forsythia* wild-type and Gtf-deficient mutants was assessed in the mixed PBMC culture. Whole PBMCs stimulated with 50 ng/ml LPS (*E. coli* O111:B4 LPS, Merck, Darmstadt, Germany) and  $10^3$  U/ml human recombinant IFN- $\gamma$  (PeproTech, Rocky Hill, NJ, United States) served as positive controls. T cell proliferation was calculated as percentage CFSE negative cells of CD3<sup>+</sup> cells after 8 days of co-culture (Lyons and Parish, 1994). T cell activation was measured via expression

of CD25 ( $\alpha$ -CD25; BD Pharmingen) by flow cytometry. CD4<sup>+</sup> T cell differentiation ( $\alpha$ -CD4; eBiosciences) was assessed by expression of signature transcription factors for Treg (FoxP3; BD Pharmingen) and Th17 (ROR $\gamma$ T; eBiosciences) cells as measured by flow cytometry. Th1 differentiation was assessed by expression of the signature transcription factor T-bet ( $\alpha$ -Tbet; eBiosciences) as measured by flow cytometry.

Data analysis was made using the Student's *t*-test, as appropriate. A *p*-value below 0.05 was considered to indicate statistical significance.

## RESULTS

### Genomic Organization of the General Protein O-Glycosylation Gene Cluster of the *T. forsythia* Type Strain

Previously, a partial protein O-glycosylation gene locus (Posch et al., 2011; Coyne et al., 2013) as well as genes for the biosynthesis of CMP-Pse, which is the activated form of this sugar acid required for its incorporation into the S-layer glycan, (Friedrich et al., 2017), were identified in the genome of *T. forsythia* ATCC 43037. That genomic region (Friedrich et al., 2015) was now investigated *in silico* for the presence of further genes with functional annotations as carbohydrate-active enzymes. This revealed a 27-kb protein O-glycosylation gene cluster (Figure 1B). From the 5' end, the gene cluster starts with a *wzx* flippase-like gene (*Tanf\_01180*) which is followed by the six genes required for the biosynthesis of CMP-Pse (Friedrich et al., 2017), present in the order *pseB* (*Tanf\_01185*), *pseC* (*Tanf\_01190*), *pseF* (*Tanf\_01200*), *pseH* (*Tanf\_01225*), *pseG* (*Tanf\_01235*), *pseI* (*Tanf\_01240*). ORFs encoding hypothetical proteins of unknown function (HP) intercept this region. Downstream, five genes encoding proteins with Gtf domains (*Tanf\_01245*, *Tanf\_01260*, *Tanf\_01290*, *Tanf\_01300*, *Tanf\_01305*, named *gtfS*, *gtfM*, *gtfI*, *gtfL*, and *gtfE*) are present. The corresponding glycosyltransferases GtfS (445 amino acids), GtfM (382 amino acids), GtfI (402 amino acids; GT1 family of Gtfs) and GtfL (420 amino acids; GT1 family of Gtfs) exhibit homology to the GT-B type superfamily of Gtfs, while GtfE (255 amino acids; GT2 family of glycosyltransferases) exhibits homology to the GT-A type superfamily.

Further downstream, *WecC* (*Tanf\_01280*, UDP-N-acetylmannosaminuronic acid dehydrogenase) and *WecB* (*Tanf\_01285*, UDP-N-acetylglucosamine 2-epimerase) are encoded, predicted to be involved in the biosynthesis of UDP-N-acetylmannosaminuronic acid. The conserved AnsB domain of *Tanf\_01265* (605 amino acids; predicted asparagine synthetase B) indicates amidotransferase activity of this ORF, putatively involved in the formation of the acetamidino (Am) modification on the C-5 at the Pse residue. A candidate gene for the glyceroyl (Gra) modification at the C-7 of Pse remains elusive. Additionally, within the protein O-glycosylation gene cluster, three genes were identified sharing similarities with SAM-dependent MtfS; these are *Tanf\_01250*, *Tanf\_01255* and *Tanf\_01295*, encoding proteins named MtfJ (90 amino acids), MtfO (167 amino acids), and MtfY (213 amino acids),

respectively. SAM-dependent domains are present in all of these MtfS; the typical glycine-rich sequence (motif I; E/DXGXGXG) (Martin and McMillan, 2002; Schubert et al., 2003) is only found within the amino acid sequence of MtfJ.

Inspection of eight further ORFs distributed over the entire protein O-glycosylation gene cluster, i.e., *Tanf\_01195*, *Tanf\_01205*, *Tanf\_01210*, *Tanf\_01220*, *Tanf\_01225*, *Tanf\_01230*, *Tanf\_01270*, and *Tanf\_01275*, did not provide evidence for functions related to carbohydrate metabolism. Thus, these genes were regarded as irrelevant for the present study.

### Transcription Analysis of the Protein O-Glycosylation Gene Cluster

To analyze whether the genes encoded by the protein O-glycosylation gene cluster are transcriptionally linked, total RNA from *T. forsythia* ATCC 43037 cells was extracted and co-transcription of the relevant genes was analyzed using RT-PCR as outlined in Supplementary Figure S1. PCR products of the expected sizes were obtained with primer pairs (Supplementary Table S2) designed to bridge the ends between the ORFs of adjacent genes, yielding amplification products only when co-transcription was occurring. The results revealed that the cluster is transcribed as a polycistronic unit spanning at least the *Tanf\_01180* to *Tanf\_01305* genes (Supplementary Figure S1). This implicates that a previously described three-gene "exopolysaccharide synthesis operon" spanning *Tanf\_01280* to *Tanf\_01290* (Honma et al., 2007) is part of the contiguous transcription unit of the *T. forsythia* ATCC 43037 protein O-glycosylation gene cluster.

### The General Protein O-Glycosylation Gene Cluster Is a Common Feature of Pathogenic *T. forsythia* Strains

The species-wide conservation of the general protein O-glycosylation gene cluster was assessed by sequence comparison of the ATCC 43037 type strain with six other publicly available *T. forsythia* genomes (*T. forsythia* UB20, FDC 92A2, UB4, KS16, UB22, and 3313; genome accessions are listed in Supplementary Table S1). Prior to that, it was confirmed by sequence homology searches, that all of these genomes possessed orthologs of the ATCC 43037 S-layer genes *tfsA* (*Tanf\_03370*) and *tfsB* (*Tanf\_03375*), which are the most abundant glycosylation targets in *T. forsythia* (Supplementary Table S5).

In all of the analyzed *T. forsythia* genomes, general protein O-glycosylation gene clusters of comparable size, content, and organization were identified (Figure 2). The major difference found between the analyzed gene clusters was in the alternate presence of six genes encoding the biosynthesis pathway for either CMP-Pse (*pseBCHGIF* in strains ATCC 43037 and UB20) or CMP-Leg (*legBCHGIF* in strains FDC 92A2, UB4, KS16, and UB22), respectively. In all cases, the corresponding genes are located immediately downstream of a conserved *wzx*-flippase like gene (*Tanf\_01180* in strain ATCC 43037). Strain 3313 presents a unique situation, since most components of the CMP-Leg pathway were found, however, *legF* could not be identified and for *legH* only a match at 29% sequence identity



(covering 95% of the sequence) could be detected. These data leave a prediction of the type of nonulosonic acid in this strain open, if present at all. Furthermore, 10 genes of unknown function that do not have counterparts in the other *T. forsythia* protein O-glycosylation gene clusters are present in that region of the 3313 genome. Apart from this difference, the region further downstream shares a high degree of similarity with the other protein O-glycosylation gene clusters. This region encodes five predicted glycosyltransferases (GtfSMILE), two UDP-N-acetylmannosaminuronic acid biosynthesis enzymes (WecB, WecC), and the putative carbohydrate modifying enzyme AsnB (Figure 2), as described above for *T. forsythia* ATCC 43037. With regard to the three MtfS (MtfJOY) predicted for the type strain, no *mtfj* gene was annotated in strain UB22. In strain 3313, a single gene was annotated at the location of *mtfj* and *mtfO*, showing sequence homology to both *mtfj* (93% of its length) and *mtfO* (entire length), suggesting either misannotation or a fused *mtfj*-*mtfO* gene. All CMP-Leg synthesizing strains contained an additional predicted Mtf gene (named *mtfX*) which does not share sequence homology to the MtfS MtfJOY. In strain FDC 92A2, there is a transposable element present between the *gtfI* and *mtfY* genes.

In contrast, the genome sequence of *Tannerella* sp. HOT-286 (phylogroup BU063; genome accession NZ\_CP017038.1), which is described as a periodontal health-associated isolate (Beall et al., 2014), showed sequence homology to only the *wzx* flippase-like gene (46% sequence identity) and the Gtf gene *gtfE* (69% sequence identity). Apart from weak matches to the *wecB* and *wecC* genes, there was no further homology to genes found in the protein O-glycosylation gene cluster of pathogenic *T. forsythia* strains. Instead, two genes with predicted Gtf domains (locus tags: BCB71\_RS10435 and BCB71\_RS10420), which are different from the *gtfSMILE* genes mentioned before, were found in that region of the HOT-286 (phylogroup BU063) genome (Figure 2). Further research on this difficult-to-grow *Tannerella* sp. (Vartoukian, 2016) is needed to assess its glycosylation potential and potential role in periodontal health and disease.

## Glycosyltransferases of the Protein O-Glycosylation Gene Cluster Assemble the Species-Specific Glycan

To investigate the principal involvement of the predicted GtfS GtfSMILE in the biosynthesis of the *T. forsythia* ATCC 43037 S-layer O-glycan, single gene knock-out mutants of the corresponding genes, i.e., *Tanf\_01260* (*gtfM*), *Tanf\_01290* (*gtfI*), *Tanf\_01300* (*gtfL*) and *Tanf\_01305* (*gtfE*), were created (Supplementary Figures S2–S5) -  $\Delta$ *Tanf\_01245* ( $\Delta$ *gtfS*) was available from a previous study (Tomek et al., 2017) - and analyzed by SDS-PAGE and Western-blotting. In comparison to the *T. forsythia* ATCC 43037 wild-type, in which the glycosylated S-layer proteins TfsA and TfsB migrate on the SDS-PAGE gel at ~230 kDa (calculated MW of the protein, 135 kDa) and ~270 kDa (calculated MW of the protein, 152 kDa), respectively, each Gtf-deficient mutant experienced a downshift of these prominent *T. forsythia* glycoproteins (Figure 3A). Downshifted S-layer glycoproteins suggest a stepwise truncation of the O-glycan from

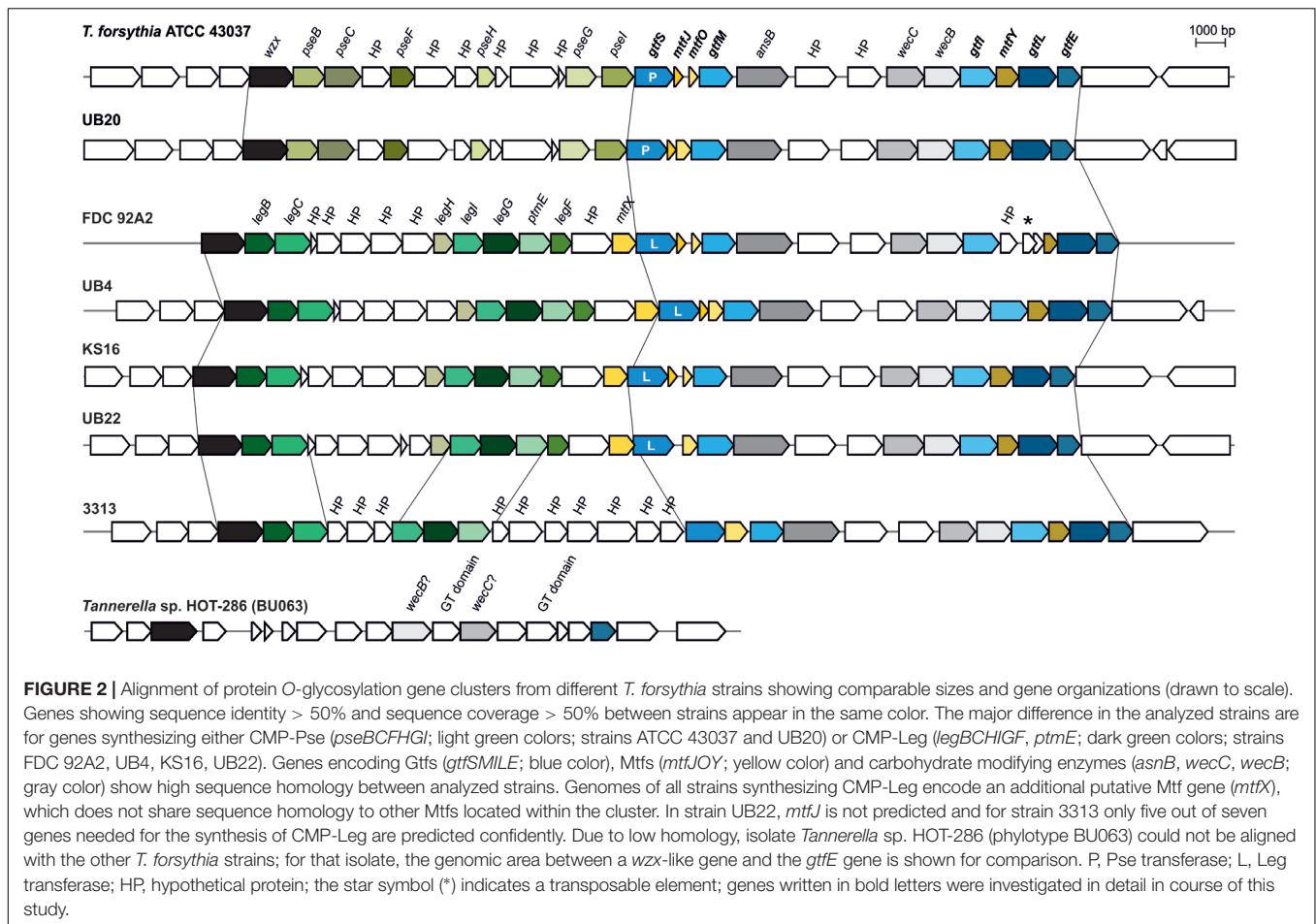
wild-type via  $\Delta$ *gtfS*,  $\Delta$ *gtfM*,  $\Delta$ *gtfI*,  $\Delta$ *gtfL* to  $\Delta$ *gtfE*. Western-blotting probed with  $\alpha$ -TfsA and  $\alpha$ -TfsB antiserum confirmed the identity of the S-layer glycoproteins in *T. forsythia* wild-type and mutant strains, with the S-layer glycoproteins of the reconstituted mutants regaining their native SDS-PAGE migration profile (Figure 3B). MS analysis of  $\beta$ -eliminated TfsB O-glycans from the Gtf mutants upon complementation with the native gene (*T. forsythia*  $\Delta$ *gtfM*<sup>+</sup>, *T. forsythia*  $\Delta$ *gtfI*<sup>+</sup>, *T. forsythia*  $\Delta$ *gtfL*<sup>+</sup>, and *T. forsythia*  $\Delta$ *gtfE*<sup>+</sup>) confirmed the synthesis of the native decasaccharide (Supplementary Figure S9). Data for *T. forsythia*  $\Delta$ *gtfS*<sup>+</sup> were published previously (Tomek et al., 2017).

To obtain insight into the specificity of the GtfS GtfSMILE in the biosynthesis of the *T. forsythia* O-glycan, ESI-MS analysis of  $\beta$ -eliminated O-glycans from TfsB (Figure 3C) and TfsA (data not shown) as present in the  $\Delta$ *gtfS*,  $\Delta$ *gtfM*,  $\Delta$ *gtfI*,  $\Delta$ *gtfL*, and  $\Delta$ *gtfE* mutants was performed. The doubly charged wild-type decasaccharide exhibited an  $m/z = 949.9$  [M+2H]<sup>2+</sup>, which corresponds to  $m/z = 1898.8$  when calculating the singly charged form thereof, confirming the composition of the previously elucidated O-glycan structure (Posch et al., 2011) (Figure 3C, i). Structure-wise, the position of the branching Fuc residue that has remained ambiguous from our initial investigations could now be determined, using a  $\Delta$ *gtfL* mutant ( $\Delta$ *Tanf\_01300*) (see below).

In comparison to the wild-type, the signal for the largest glycan produced by a  $\Delta$ *gtfS* ( $\Delta$ *Tanf\_01245*) mutant was detected at  $m/z = 1523.4$  [M+H]<sup>+</sup>, which agrees with the  $m/z$  value of the *T. forsythia* O-glycan lacking the terminal Pse5Am7Gra residue (361.2 Da) and one methyl group (14.0 Da). A detailed analysis of the GtfS protein was performed recently in our group and revealed that it has  $\alpha$ -2,4 Pse5Am7Gra transferase activity (Tomek et al., 2017) (Figure 3C, ii). The  $\Delta$ *gtfM* mutant ( $\Delta$ *Tanf\_01260*) lacks the 4-O-methyl-N-acetylmannosaminuronic acid residue (231.1 Da) in addition to Pse5Am7Gra, making the signal at  $m/z = 1306.4$  [M+H]<sup>+</sup> the largest detectable glycan for this mutant (Figure 3C, iii). The MS data together with the *T. forsythia* ATCC 43037 O-glycan structure (compare with Figure 1A) are, therefore, indicative of GtfM having a  $\beta$ -1,3-N-acetylmannosaminuronic acid transferase activity. The glycan is further truncated upon knocking-out of *gtfI* ( $\Delta$ *Tanf\_01290*). In this mutant glycan, the three-sugar branch composed of the Pse5Am7Gra, an N-acetyl mannosaminuronic acid and the 4-O-methyl-N-acetyl mannosaminuronic acid residue (in total 809.1 Da), is absent and results in a signal corresponding to the ammonium adduct ion at  $m/z = 1106.4$  [M+NH<sub>4</sub>]<sup>+</sup> (Figure 3C, iv). Thus, the proposed enzymatic function of GtfI is that of a  $\beta$ -1,4-N-acetylmannosaminuronic acid transferase.

The  $m/z = 930.3$  [M+NH<sub>4</sub>]<sup>+</sup> signal of a  $\Delta$ *gtfL* mutant ( $\Delta$ *Tanf\_01300*) could initially not be assigned to the published O-glycan structure (Posch et al., 2011). In our previous study, a fragment ion of  $m/z = 341.0$  was tentatively interpreted as the single cleavage C-ion Fuc-MeGal. However, the  $m/z = 930.3$  glycan of the  $\Delta$ *gtfL* mutant, which contains two fucoses and lacks the distal Gal, necessitated another interpretation of this fragment (Figure 4), leading to a reconsideration of the location of the second fucose residue. Inspection of the fragment spectrum of  $m/z = 930.3$ <sup>1+</sup> revealed an  $m/z = 329.0$  fragment not present





in the monofucosylated  $m/z = 784.6^{1+}$  peak (Figure 4). This  $Y_{1\beta}Y_{1\gamma}$  double cleavage ion strongly indicated that a Fuc residue is attached to the reducing-end Gal. This interpretation was supported by the fragment ion  $m/z = 651.1$ , which was observed in the product ion spectra of  $m/z = 930.3^{1+}$ . Thus, these findings prove that the glycan of this mutant is composed of the six innermost sugar residues, and that GtfL acts as an  $\alpha$ -1,2 galactosyltransferase (Figures 1A, 3C, v). Simultaneously,  $\beta$ -1,4 *N*-acetylmannosaminuronic acid transfer activity of GtfI seems to be affected by the deletion of GtfL, since the *Pse*5Am7Gr-containing trisaccharide branch is also missing in this structure, indicating the requirement of either a distinct composition of the acceptor for recognition by the enzyme or the necessity of association of GtfI with GtfL for enzymatic activity. Finally, fucosyltransferase activity of GtfE is supported by the analysis of a  $\Delta$ *gtfE* knock-out mutant ( $\Delta$ *Tanf\_01305*) which reveals an ammonium adduct mass of  $m/z = 784.2$   $[M+NH_4]^+$  that represents an O-glycan composed of the five innermost sugar residues (pentasaccharide core) (Figure 3C, vi).

These data are complemented by previous results from our group showing that the O-glycan from a *wecC* knock-out mutant ( $\Delta$ *Tanf\_01280*) lacks the same three-sugar branch as the  $\Delta$ *gtfI* mutant (Posch et al., 2011). We concluded that *WecC* fulfills its predicted role as a UDP-*N*-acetylmannosaminuronic

acid dehydrogenase which works in concert with the predicted UDP-*N*-acetylglucosamine 2-epimerase *WecB* (*Tanf\_01285*) to synthesize UDP-*N*-acetylmannosaminuronic acid prior to its transfer to the branching Fuc residue of the *T. forsythia* O-glycan structure (compare with Figure 1A), catalyzed by GtfI (Figure 3C, iv).

Summarizing, the *T. forsythia* protein O-glycosylation gene cluster encodes all necessary information for the assembly of the species-specific portion of the deca-saccharide.

### Three Methyltransferases Modify the O-Glycan With Two Methyl Groups

While two methylated sugars are present in the *T. forsythia* ATCC 43037 O-glycan structure, three putative Mtfs are encoded within the protein O-glycosylation gene cluster (*MtfJOY*). To test the methylation activity and specificity of these predicted enzymes, single gene knock-outs were constructed (Supplementary Figures S7–S9). O-Glycans of mutants, deficient in either the Mtf gene *mtfJ* ( $\Delta$ *Tanf\_01250*) or *mtfO* ( $\Delta$ *Tanf\_01255*), experienced a loss of the 4-*O*-methyl group at the terminal *N*-acetylmannosaminuronamide, as MS analyses revealed (Figure 5; red circles indicate the absence of the methyl groups). The expected loss of 14 Da resulted in a doubly charged ion at  $m/z = 942.9$

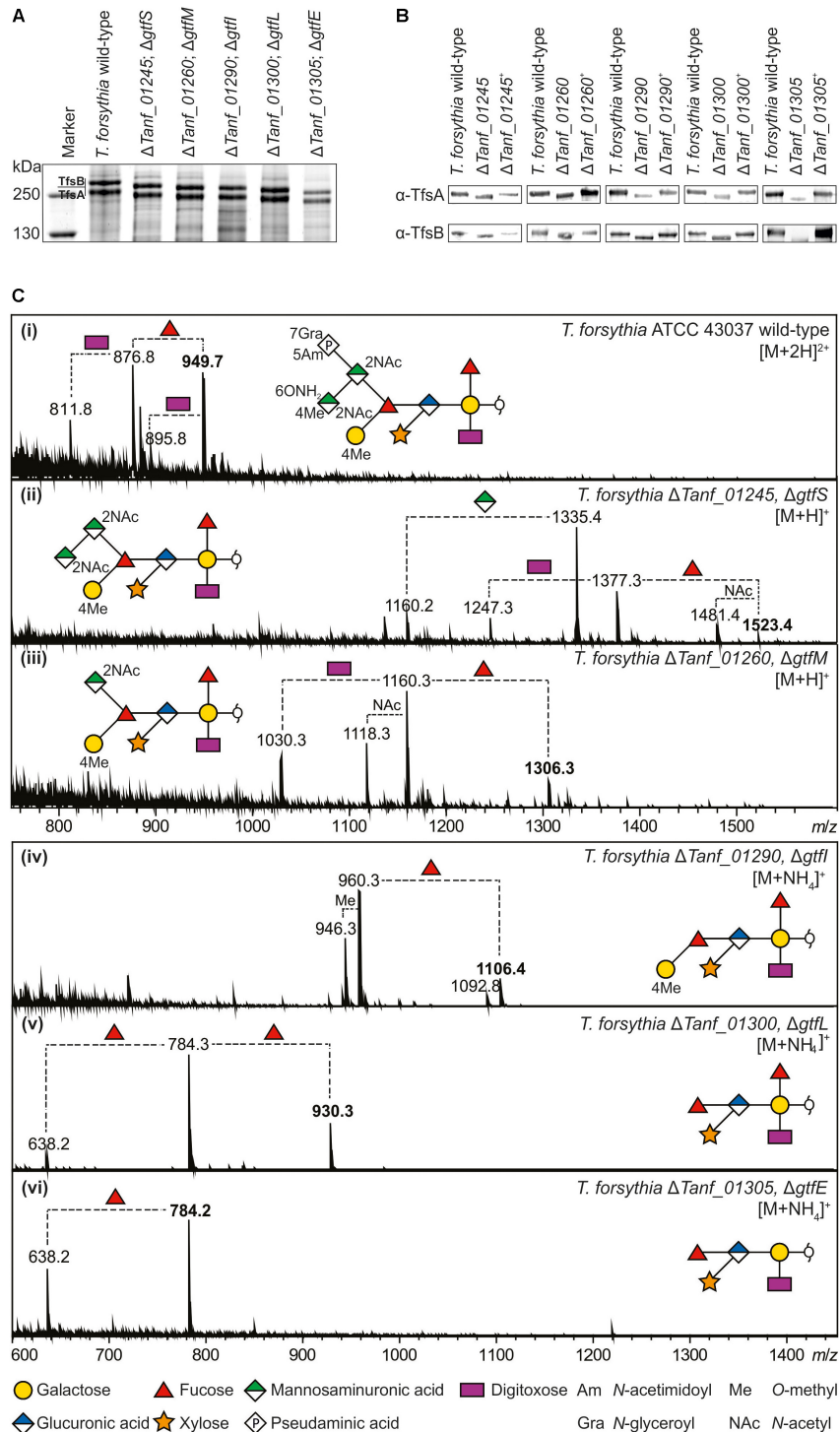
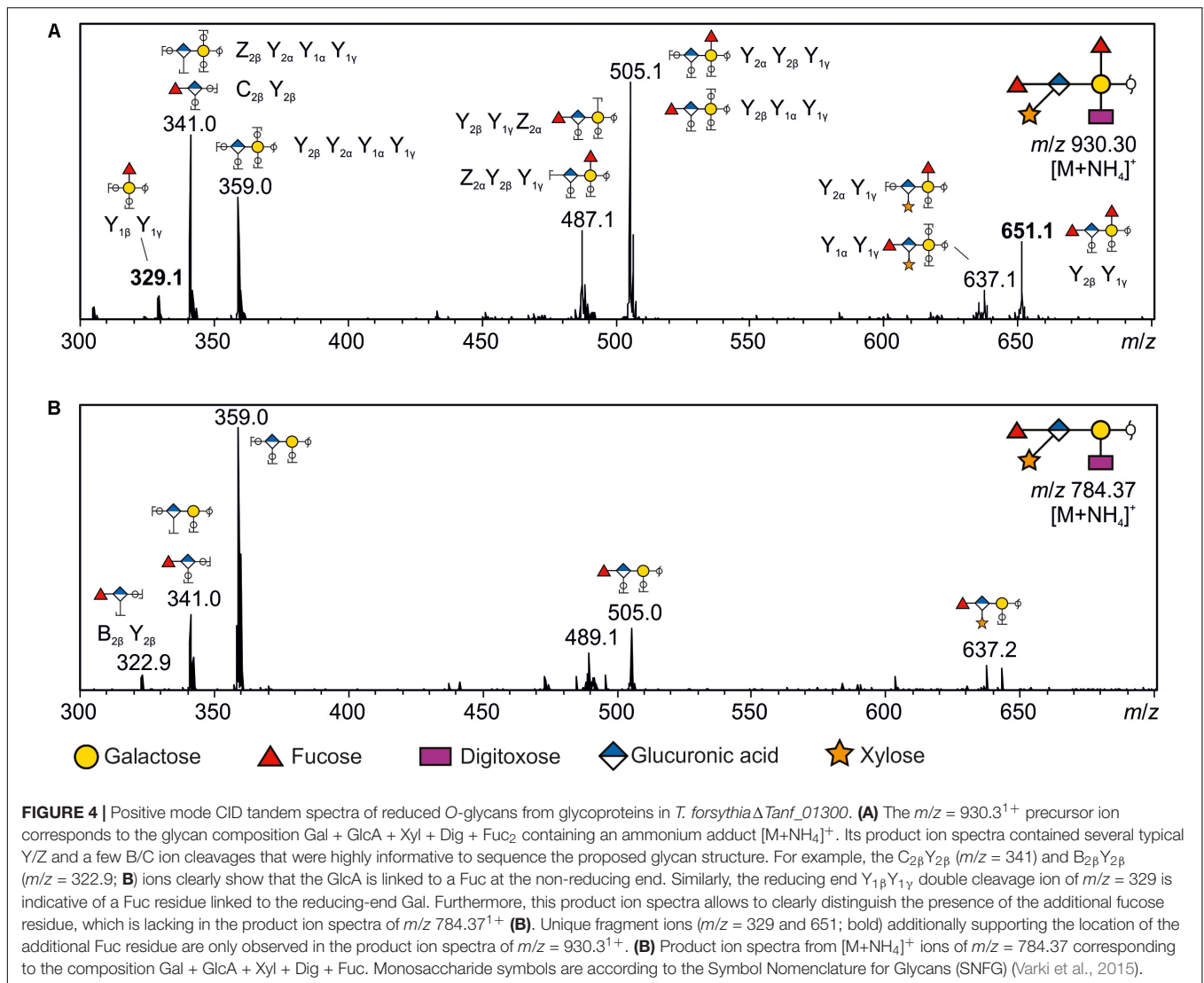


**FIGURE 3 | (A)** Coomassie Brilliant Blue staining of crude cell extracts from *T. forsythia* ATCC 43037 wild-type and glycosyltransferase-deficient mutants after separation on a 7.5% SDS-PA gel. The S-layer glycoproteins (labeled TfsA and TfsB) are indicated and the downshifts resulting from glycan truncation can be seen in the mutants. S-layer glycoprotein bands were further processed for MS analyses. PageRuler Plus Prestained Protein Ladder (Thermo Fisher Scientific) was used as a protein molecular weight marker. **(B)** Western-blots probed with  $\alpha$ -TfsA and  $\alpha$ -TfsB antiserum for confirmation of the identity of S-layer glycoproteins. Glycoproteins from all glycosyltransferase-deficient mutants ( $\Delta$ gtfSMILE) experienced a downshift resulting from glycan truncation, whereas the reconstituted strains (denoted with +) regained wild-type migration, indicating the presence of the complete mature glycan, proving successful recombination. **(C, i-vi)** ESI-MS sum spectra of  $\beta$ -eliminated TfsB O-glycans from *T. forsythia* wild-type and mutants. The glycan structures of the signals corresponding to the largest mass (bold *m/z* values) are shown in SNFG representations (Varki et al., 2015). O-Glycan signals detected for the respective mutants were assigned based on the *m/z* mass differences corresponding to the loss of individual sugar units and/or modifications.



$[M+2H]^{2+}$  as detected for the analyzed TfsB (**Figure 5**) and TfsA (data not shown) O-glycans of either Mtf mutant. While Mtfj and MtfO obviously catalyze methyl transfer to the same sugar residue, these proteins differ in length and do not share significant sequence similarity. In contrast, the O-glycan of the  $\Delta$ mtfY mutant ( $\Delta$ Tanf\_01295) lacked the 4-O-methyl group on the distal Gal residue (**Figure 5**). The discrimination which of the two methyl groups was affected in the different Mtf mutants was inferred from the occurrence of unique glycan fragments obtained during MS and MS/MS analyses (data not shown).

## Protein Glycosylation Affects Immunogenicity of *T. forsythia*

We proceeded to investigate whether differential cell surface protein O-glycosylation as present in the Gtf-deficient mutants of *T. forsythia* ATCC 43037 impacts the bacterium's overall immunogenicity. For this endeavor, we selected two mutants with distinct O-glycan compositions for which we expected

differential responses of infected immune cells in comparison to the wild-type. This included  $\Delta$ gtfS, lacking the sialic acid mimic Pse5Am7Gra (Tomek et al., 2017) and  $\Delta$ gtfE (this study) producing the pentasaccharide core only and, thus, exposing a terminal Fuc residue. Further,  $\Delta$ gtfI which produces the same truncated glycan as  $\Delta$ wecC ( $\Delta$ Tanf\_01280) (Posch et al., 2011) was included as a control, since for that mutant reference immunology data is available in the literature (Settem et al., 2013).

Dendritic cells as central communicators linking innate and adaptive immune responses possess a wide variety of PRRs that allow them to recognize and quickly respond to the presence of opportunistic pathogens (Reis e Sousa, 2006; Merad et al., 2013). The high selectivity of these PRRs enables DCs to fine-tune the outcome of the immune response, depending on the molecular characteristics of the stimulus (Lutz and Schuler, 2002). Therefore, BMDCs and human monocyte-derived DCs were used to explore how the loss of certain sugar residues of the *T. forsythia* O-glycan affects activation and release of



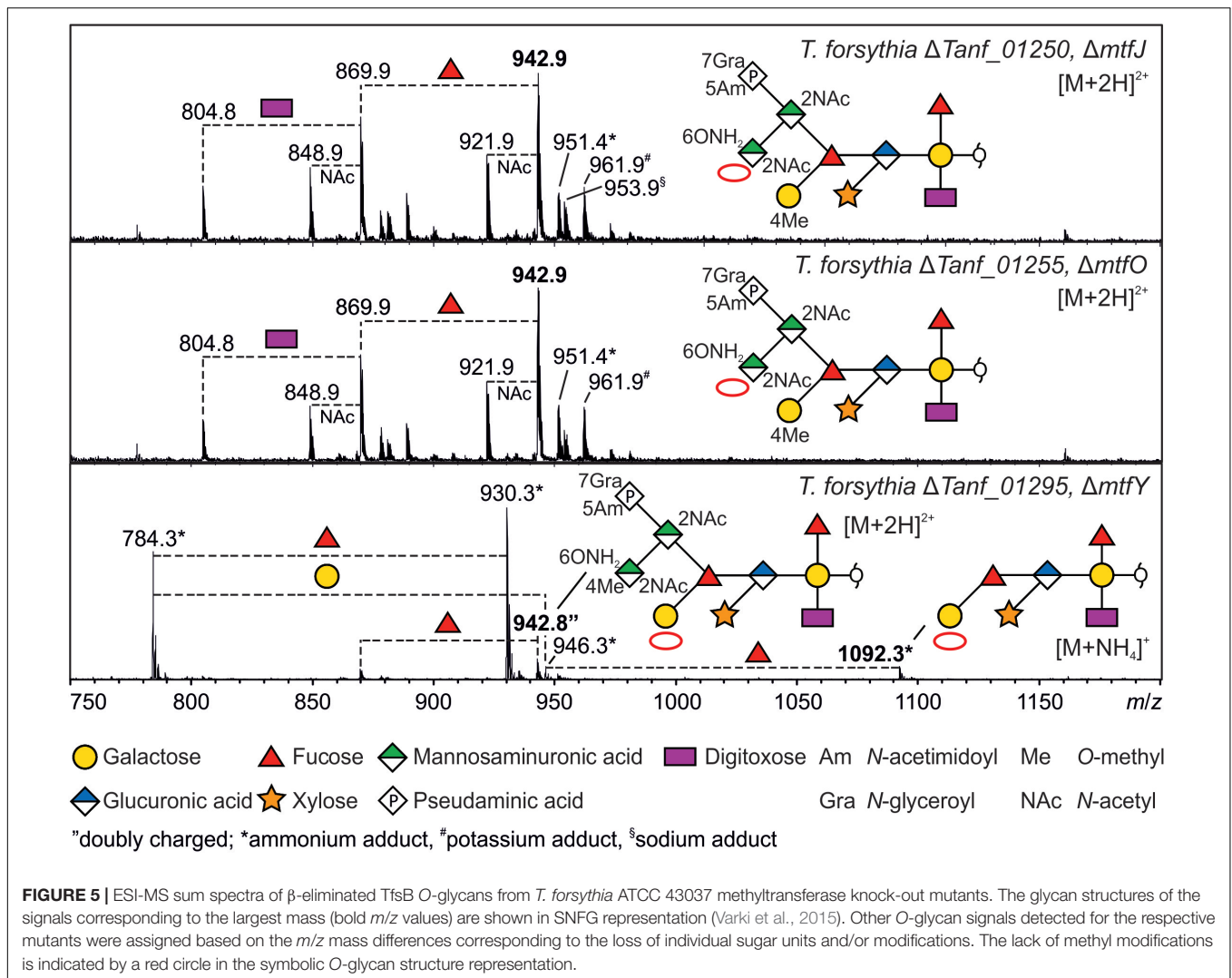


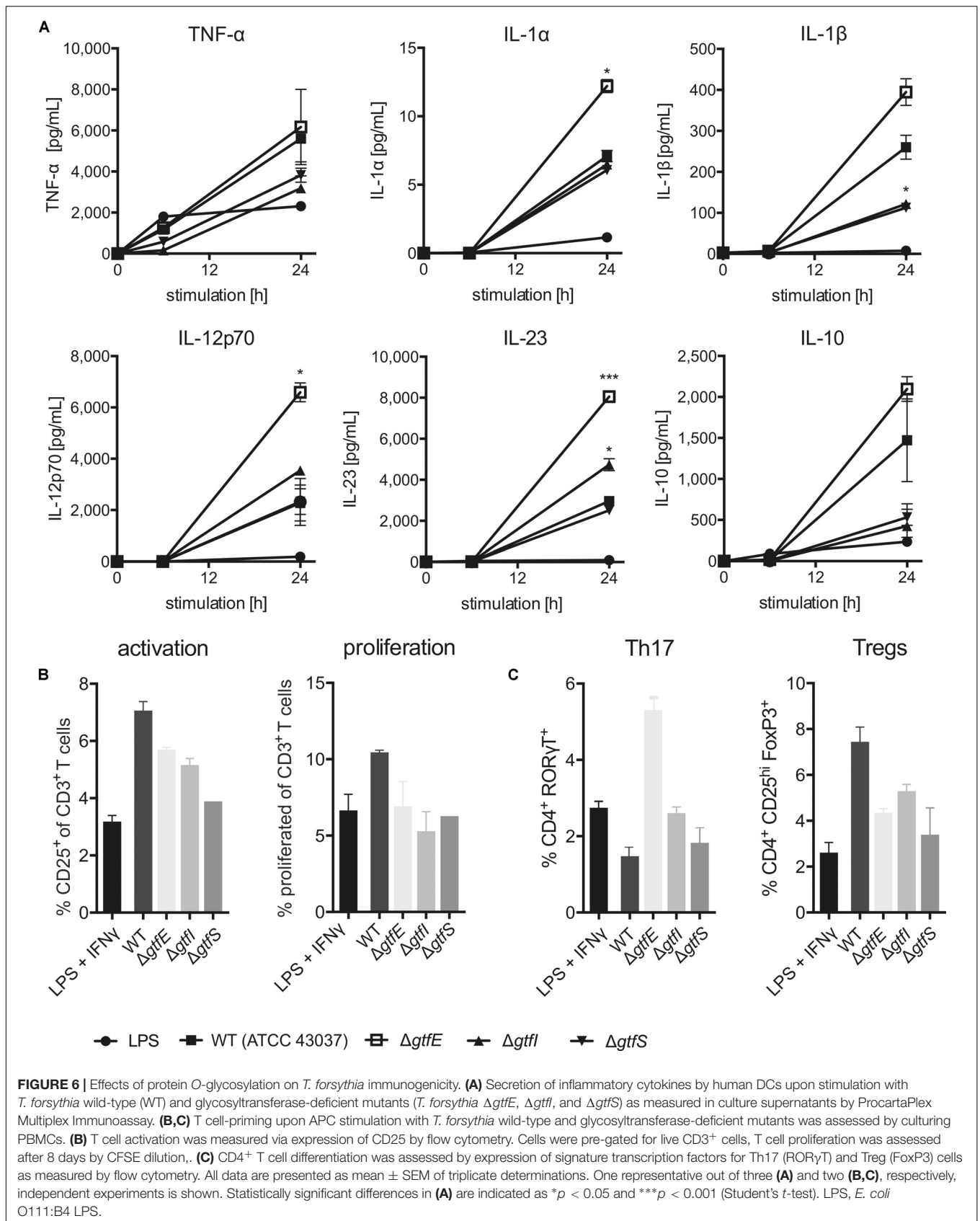
**FIGURE 5** | ESI-MS sum spectra of  $\beta$ -eliminated TfsB O-glycans from *T. forsythia* ATCC 43037 methyltransferase knock-out mutants. The glycan structures of the signals corresponding to the largest mass (bold  $m/z$  values) are shown in SNFG representation (Varki et al., 2015). Other O-glycan signals detected for the respective mutants were assigned based on the  $m/z$  mass differences corresponding to the loss of individual sugar units and/or modifications. The lack of methyl modifications is indicated by a red circle in the symbolic O-glycan structure representation.

inflammatory cytokines by these cells as well as the subsequent polarization of an adaptive T cell response.

First, the surface expression of DC maturation markers, including MHC-II, CD80 and CD86, upon stimulation by *T. forsythia* wild-type and the  $\Delta$ gtfS,  $\Delta$ gtfI, and  $\Delta$ gtfE mutants was investigated. Over a period of 24 h, all of these activation markers were up-regulated in response to stimulation and did not reveal any differences between the tested strains (**Supplementary Figure S10A**). As this suggested no effect on the overall activation of DCs, their functionality was tested next. While secretion of most pro-inflammatory cytokines was not altered between the wild-type and the Gtf-deficient mutants,  $\Delta$ gtfE resulted in a profound increase in IL-1 $\beta$ , IL-12, and IL-23 release by human monocyte-derived DCs over 24 h post-stimulation (**Figures 6A** and **Supplementary Figure S10B**), and in TNF- $\alpha$  and IL-6, as observed with mouse-derived DCs (**Supplementary Figure S11**). Striking differences were observed with regard to IL-1 $\beta$  production; while  $\Delta$ gtfE enhanced secretion of this key inflammatory cytokine in human DCs,  $\Delta$ gtfI and  $\Delta$ gtfS yielded a significant decrease when compared to the wild-type (**Figure 6A**).

A similar effect was observed for IL-10 (**Figure 6A**), which acts as an important immunosuppressive mediator and is required to dampen ongoing inflammatory responses.

These results prompted us to explore the T cell-priming potential of antigen-presenting cells (APCs) upon stimulation by different *T. forsythia* glycosylation mutants. We therefore cultured PBMCs, containing APCs and T cells, for 8 days in the presence of different *T. forsythia* strains. With regard to both activation (CD25 up-regulation) and proliferation, a decline in T cell activation upon stimulation with all Gtf-deficient mutants as compared to the wild-type could be observed (**Figure 6B**). However, dissecting the polarization of the resulting T cell response, we observed a remarkable induction of ROR $\gamma$ T-expressing CD4<sup>+</sup> T cells by  $\Delta$ gtfE-stimulated DCs, whereas only a minor effect was seen for the other tested strains (**Figure 6C**). This suggests a trend toward enhanced differentiation of Th17 cells in response to *T. forsythia* glycan truncation, an effect that has been previously reported to be of relevance for the progression of periodontitis (Settem et al., 2013). Critically, this observation is reinforced by the profound increase in IL-23



and IL-1 $\beta$  we found upon human DC stimulation with  $\Delta$ *gftE* (Figure 6A), as these cytokines represent key mediators of Th17 polarization (Iwakura and Ishigame, 2006; Sutton et al., 2009). The differentiation of Tregs was similarly reduced by all truncated glycans in comparison to the wild-type (Figure 6C), indicating an overall involvement of the O-glycan in maintaining a suppressive T cell environment. Moreover, a minor trend toward decreased induction of Th1 (IFN- $\gamma$ <sup>+</sup>) cells could be observed (Supplementary Figure S10C), which corresponds to a slightly reduced IFN- $\gamma$  secretion by human DCs stimulated with *T. forsythia* Gtf-deficient mutants (Supplementary Figure S10B).

## DISCUSSION

Periodontitis is an inflammatory disease that is highly prevalent among the adult population world-wide. It involves the periodontal pathogens *T. forsythia*, *Porphyromonas gingivalis*, and *Treponema denticola*, together constituting the so-called “red complex” of bacteria (Kassebaum et al., 2014; Hajishengallis, 2015). In *T. forsythia*, the prominent and unique S-layer glycoproteins TfsA and TfsB are virulence factors (Sharma, 2010). While previous studies were designed to elucidate the S-layer O-glycan structure (Posch et al., 2011; Friedrich et al., 2017), the S-layer ultrastructure (Sekot et al., 2012; Oh et al., 2013), and the immunological properties of the S-layer glycoproteins (Yoneda et al., 2003; Sakakibara et al., 2007; Sekot et al., 2011; Chinthamani et al., 2017), only few data is available on the impact of *T. forsythia*'s cell surface glycosylation on the modulation of host immunity (Settem et al., 2013, 2014). This is surprising given the fact that *T. forsythia* O-glycans are highly abundant on the bacterial cell surface due to their display via the S-layer matrix (Sekot et al., 2012), making them prone to act at the bacterium-immune interface.

To provide a basis for validating *T. forsythia*'s S-layer protein O-glycosylation as a possible target against periodontitis, within the frame of this study (i) the prevalence of an underlying protein O-glycosylation gene cluster in the genomes of different *T. forsythia* strains was assessed, (ii) insights into the O-glycan biosynthesis pathway were obtained, and (iii) a relationship between O-glycan structure and immunogenicity was delineated.

In this study, the general protein O-glycosylation gene cluster of *T. forsythia* ATCC 43037 was extended to span 27-kb on the bacterium's genome (Friedrich et al., 2015). For 18 out of the 26 ORFs, carbohydrate metabolism-related functions were predicted. These include, a Wzx-like flippase for translocation of the glycan moiety to the periplasmic space prior to protein transfer, six enzymes needed for the synthesis of CMP-Pse (PseBCFHGI) as well as two enzymes for the synthesis of UDP-linked N-acetyl mannosaminuronic acid (WecB, WecC), five Gtfs (GtfSMILE), three MtfS (MtfJOY), and one ORF putatively involved in the Am-modification of the Pse residue (Figure 1B).

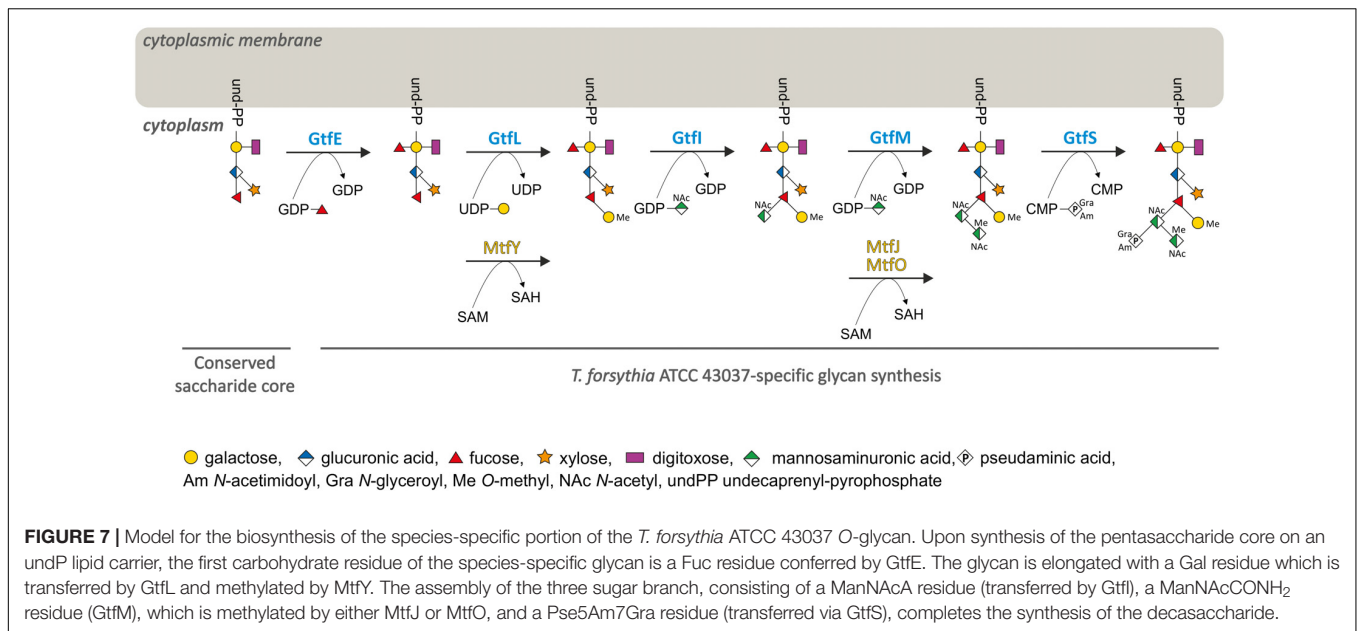
Genome comparisons of *T. forsythia* strains revealed that all seven strains included in this study have the genetic potential for protein O-glycosylation (Figure 2). A high degree of conservation of the protein O-glycosylation gene clusters with regard to content and organization of genes became evident, with a

possible grouping of strains according to the type of terminal nonulosonic acid synthesized (Pse versus Leg), with only one strain presenting an ambiguous situation. As a common feature, the O-glycosylation gene clusters in all analyzed strains start with orthologs of the Gtf genes *gftE* (*Tanf\_01305*) and *gftL* (*Tanf\_01300*) and terminate with an ortholog of the flippase gene *wzx* (*Tanf\_01180*), which is identical to the situation found in 24 other *Bacteroides* species (Coyne et al., 2013). While orthologs of *wzx* and *gftE* are also predicted in the genome of the periodontal health-associated isolate *Tannerella* sp. HOT-286 (Beall et al., 2014), none of the intervening genes related to carbohydrate metabolism as present in the pathogenic strains are confidently predicted. Thus, it is conceivable that the potential of complex protein O-glycosylation is a specific trait of periodontitis-associated *T. forsythia* strains, especially when considering that cell surface glycosylation in bacteria can modulate immune responses during pathogenesis (Szymanski and Wren, 2005; Lebeer et al., 2010; Valguarnera et al., 2016).

Experimentally, we have determined the roles of five Gtfs and three MtfS encoded in the protein O-glycosylation gene cluster by analysing the protein-released glycans of the respective knock-out mutants. We could establish an assembly line for the *T. forsythia*-specific portion of the O-glycan by subsequent involvement of the Gtfs GtfELIMS (Figure 7). While the underlying genetic information is encoded in the gene cluster, the information for the assembly of the pentasaccharide core would be encoded elsewhere on the bacterial genome. A putative O-OTase transferring the glycan onto the acceptor proteins could not be identified for *T. forsythia*, so far. This leaves the question open of whether this O-glycan is synthesized by an OTase-dependent or OTase-independent mechanism (Choi et al., 2010; Grass et al., 2010; Schwarz et al., 2011; Iwashkiw et al., 2013). Coyne et al. (2013) suggested two possible models for protein O-glycosylation in *Bacteroidetes*, exemplified with *B. fragilis*. According to the first model, the glycan core and the species-specific glycan would be built separately on an undecaprenyl-phosphate (undP) lipid carrier and flipped to the periplasmic side of the cytoplasmic membrane by individual Wzx flippases. The core glycan would be linked to the protein by an as yet unidentified OTase, followed by linking of the species-specific glycan portion to the core by an O-antigen ligase-like protein. Alternatively, the species-specific glycan might be added to the core in the cytoplasm and then a single flippase would transfer the entire glycan to the periplasm for addition to proteins (Fletcher et al., 2009; Coyne et al., 2013). Considering our experimental set-up we cannot make any conclusion as to which of the two models would be valid for *T. forsythia*.

Concerning 4-O-methylation of the distal Gal and the N-acetyl mannosaminuronamide residue, there is redundancy of enzymes, since the latter residue can be methylated by both MtfJ and MtfO, while MtfY recognizes only the distal Gal residue as a substrate. It remains to be investigated if MtfJ and MtfO might be differentially expressed in *T. forsythia* as a function of growth conditions or other signals and, generally, if methylation occurs at the nucleotide-sugar level or after sugar transfer to the nascent glycan. Methylation of bacterial glycans is a rarely reported event. Although methylation of the non-reducing-end sugar of





a nascent polysaccharide chain has been discussed as a stop-signal for glycan chain elongation (Clarke et al., 2011), a clear determination of its biological function is still missing, especially when occurring at multiple sites of the glycan (Staudacher, 2012). O-Methylated glycans were recently suggested to constitute a conserved target of the fungal and animal innate immune system (Wohlschlagler et al., 2014). All three Mtf-deficient *T. forsythia* mutants from our study might aid in defining the roles of O-methylated sugars in a bacterial context.

In the natural habitat of the oral cavity, *T. forsythia* finds itself in an area of conflict between the requirement of inflammation to procure nutrients from tissue breakdown and the necessity to evade immune-mediated killing (Settem et al., 2013, 2014). Similar to other inflammatory diseases, disruption of the proper balance between individual subtypes of Th cells contributes to the progression of periodontitis (Baker, 2000). In a previous study using a *T. forsythia*  $\Delta wecC$  glycosylation mutant (representing the same glycan structure as the  $\Delta gtfI$  mutant of the current study), it was found that truncation of the O-glycan translated into a robust Th17 response with the consequence of reduced alveolar bone loss in mice. Additionally, the  $\Delta wecC$  mutant was increasingly susceptible to neutrophil-mediated clearance. Based on these data a fundamental role of *T. forsythia* wild-type cell surface glycosylation in restraining the Th17 response and ensuring the persistence of the pathogen in the host was proposed (Settem et al., 2013). The attenuated, Th17-biasing glycosylation mutant devoid of the O-glycan's trisaccharide branch was effective in blocking *P. gingivalis* persistence in a periodontitis mouse model (Settem et al., 2014), unraveling the *T. forsythia* O-glycan as a means for influencing the pathogenesis of periodontitis. However, it is still under debate if Th17 responses have protective or destructive roles in inflammatory diseases, since this might depend on the specificity and phase of the disease (Ohshima et al., 2009).

Using *T. forsythia* mutants with defined, truncated O-glycans, we attempted to obtain clearer insight into the O-glycan structure–function relationship at the immune interface. Analysis of DC maturation markers did not reveal differential activation by the glycosylation mutants in comparison to the wild-type. In terms of release of proinflammatory cytokines by human DCs, only *T. forsythia*  $\Delta gtfE$  resulted in a profound increase in TNF- $\alpha$ , IL-6, IL-1 $\beta$ , IL-12, and IL-23 release over 24 h post-stimulation (Figures 6A and Supplementary Figure S11). Especially with the enhanced secretion of IL-1 $\beta$  and IL-23, which are key mediators of Th17 polarization (Iwakura and Ishigame, 2006; Sutton et al., 2009), this mutant showed a striking difference to  $\Delta gtfI$  and  $\Delta gtfS$  where a decrease of these cytokines was found (Figure 6A). In line with these data, also the analysis of the T cell-priming potential of APCs upon stimulation revealed *T. forsythia*  $\Delta gtfE$  as a unique stimulus. Here, a remarkable induction of ROR $\gamma$ T-expressing CD4<sup>+</sup> T cells was observed, whereas only a minor effect was seen for the other tested mutants (Figure 6C). This suggests an enhanced differentiation of Th17 cells in response to *T. forsythia* glycan truncation, which was most pronounced upon stimulation with the pentasaccharide core only. For the  $\Delta gtfI$  mutant, equaling O-glycan structure-wise the  $\Delta wecC$  mutant for which this effect had been reported before (Settem et al., 2013), a comparably minor effect was seen. We conclude that a more truncated version of the O-glycan is even more favorable for inducing a robust Th17 response. *Vice versa*, Th17 suppression is maintained regardless of the presence of the residues N-acetyl mannosaminuronic acid, N-acetyl mannosaminuronamide and Pse5Am7Gra. This implicates that the phylum-wide conserved core as present in  $\Delta gtfE$  is responsible for modulating DC effector functions by Th17 activation, while the species-specific glycan portion, either in complete or truncated form, is required for maintaining a Th17 suppressive environment. This might

contribute to *T. forsythia*'s strategy as part of a dysbiotic microbial community to resist immune elimination and create permissive conditions for growth in a nutritionally favorable environment.

## AUTHOR CONTRIBUTIONS

CS and MT conceived the study, designed the experiments, developed the methodology, and wrote the manuscript. MT, DM, MW, VF, BJ, KF, LN, IN, NZ, AE-D, and DK performed the experiments. MT, DM, NZ, JD, AE-D, DK, HH, FA, and CS analyzed the data. All authors read and approved the submitted version of the manuscript. Written informed consent was obtained from all authors of the study.

## FUNDING

This work was supported by the Austrian Science Fund FWF, projects P24317-B22 and I2875-B22 (to CS) and the Doctoral

Program "BioToP – Biomolecular Technology of Proteins" W1224. DK is the recipient of an Australian Research Council Future Fellowship (project number FT160100344) funded by the Australian Government.

## ACKNOWLEDGMENTS

The authors gratefully acknowledge St. Anna Kinderkrebsforschung, Children's Cancer Research Institute, Medical University of Vienna, Vienna, Austria, for providing access to the immunology facility.

## SUPPLEMENTARY MATERIAL

The Supplementary Material for this article can be found online at: <https://www.frontiersin.org/articles/10.3389/fmicb.2018.02008/full#supplementary-material>

## REFERENCES

- Altschul, S. F., Madden, T. L., Schaffer, A. A., Zhang, J., Zhang, Z., Miller, W., et al. (1997). Gapped BLAST and PSI-BLAST: a new generation of protein database search programs. *Nucleic Acids Res.* 25, 3389–3402. doi: 10.1093/nar/25.17.3389
- Baker, P. J. (2000). The role of immune responses in bone loss during periodontal disease. *Microbes Infect.* 2, 1181–1192. doi: 10.1016/S1286-4579(00)01272-7
- Beall, C. J., Campbell, A. G., Dayeh, D. M., Griffen, A. L., Podar, M., and Leys, E. J. (2014). Single cell genomics of uncultured, health-associated *Tannerella* BU063 (Oral Taxon 286) and comparison to the closely related pathogen *Tannerella forsythia*. *PLoS One* 9:e89398. doi: 10.1371/journal.pone.0089398
- Bloch, S., Thurnheer, T., Murakami, Y., Belibasakis, G. N., and Schäffer, C. (2017). Behavior of two *Tannerella forsythia* strains and their cell surface mutants in multispecies oral biofilms. *Mol. Oral Microbiol.* 32, 404–418. doi: 10.1111/omi.12182
- Bloch, S., Zwicker, S., Bostanci, N., Sjöling, A., Bostrom, E. A., Belibasakis, G. N., et al. (2018). Immune response profiling of primary monocytes and oral keratinocytes to different *Tannerella forsythia* strains and their cell surface mutants. *Mol. Oral Microbiol.* 33, 155–167. doi: 10.1111/omi.12208
- Camacho, C., Coulouris, G., Avayyan, V., Ma, N., Papadopoulos, J., Bealer, K., et al. (2009). BLAST+: architecture and applications. *BMC Bioinformatics* 10:421. doi: 10.1186/1471-2105-10-421.
- Ceroni, A., Maass, K., Geyer, H., Geyer, R., Dell, A., and Haslam, S. M. (2008). GlycoWorkbench: a tool for the computer-assisted annotation of mass spectra of glycans. *J. Proteome Res.* 7, 1650–1659. doi: 10.1021/pr7008252
- Cheng, H. R., and Jiang, N. (2006). Extremely rapid extraction of DNA from bacteria and yeasts. *Biotechnol. Lett.* 28, 55–59. doi: 10.1007/s10529-005-4688-z
- Chinthamani, S., Settem, R. P., Honma, K., Kay, J. G., and Sharma, A. (2017). Macrophage inducible C-type lectin (Mincle) recognizes glycosylated surface (S)-layer of the periodontal pathogen *Tannerella forsythia*. *PLoS One* 12:e0173394. doi: 10.1371/journal.pone.0173394
- Choi, K.-J., Grass, S., Paek, S., St. Geme, J. W. III, and Yeo, H.-J. (2010). The *Actinobacillus pleuropneumoniae* HMW1C-like glycosyltransferase mediates N-linked glycosylation of the *Haemophilus influenzae* HMW1 adhesin. *PLoS One* 5:e15888. doi: 10.1371/journal.pone.0015888
- Clarke, B. R., Richards, M. R., Greenfield, L. K., Hou, D., Lowary, T. L., and Whitfield, C. (2011). *In vitro* reconstruction of the chain termination reaction in biosynthesis of the *Escherichia coli* O9a O-polysaccharide: the chain-length regulator, WbdD, catalyzes the addition of methyl phosphate to the non-reducing terminus of the growing glycan. *J. Biol. Chem.* 286, 41391–41401. doi: 10.1074/jbc.M111.295857
- Coyne, M. J., Fletcher, C. M., Chatzidaki-Livanis, M., Posch, G., Schäffer, C., and Comstock, L. E. (2013). Phylum-wide general protein O-glycosylation system of the Bacteroidetes. *Mol. Microbiol.* 88, 772–783. doi: 10.1111/mmi.12220
- Egge-Jacobsen, W., Salomonsson, E. N., Aas, F. E., Forslund, A.-L., Winther-Larsen, H. C., Maier, J., et al. (2011). O-linked glycosylation of the PilA pilin protein of *Francisella tularensis*: identification of the endogenous protein-targeting oligosaccharyltransferase and characterization of the native oligosaccharide. *J. Bacteriol.* 193, 5487–5497. doi: 10.1128/JB.00383-11
- Elhenawy, W., Scott, N. E., Tondo, M. L., Orellano, E. G., Foster, L. J., and Feldman, M. F. (2016). Protein O-linked glycosylation in the plant pathogen *Ralstonia solanacearum*. *Glycobiology* 26, 301–311. doi: 10.1093/glycob/cwv098
- Espitia, C., Servin-Gonzalez, L., and Mancilla, R. (2010). New insights into protein O-mannosylation in actinomycetes. *Mol. Biosyst.* 6, 775–781. doi: 10.1039/b916394h
- Finn, R. D., Coggill, P., Eberhardt, R. Y., Eddy, S. R., Mistry, J., Mitchell, A. L., et al. (2016). The Pfam protein families database: towards a more sustainable future. *Nucleic Acids Res.* 44, D279–D285. doi: 10.1093/nar/gkv1344
- Fletcher, C. M., Coyne, M. J., Villa, O. F., Chatzidaki-Livanis, M., and Comstock, L. E. (2009). A general O-glycosylation system important to the physiology of a major human intestinal symbiont *Bacteroides fragilis*. *Cell* 137, 321–331. doi: 10.1016/j.cell.2009.02.041
- Friedrich, V., Janesch, B., Windwarder, M., Maresch, D., Braun, M. L., Megson, Z. A., et al. (2017). *Tannerella forsythia* strains display different cell-surface nonulosonic acids: biosynthetic pathway characterization and first insight into biological implications. *Glycobiology* 27, 342–357. doi: 10.1093/glycob/cwv129
- Friedrich, V., Pabinger, S., Chen, T., Messner, P., Dewhirst, F. E., and Schäffer, C. (2015). Draft genome sequence of *Tannerella forsythia* type strain ATCC 43037. *Genome Announc.* 3:e00660-15. doi: 10.1128/genomeA.00660-15
- Gallucci, S., Lolkema, M., and Matzinger, P. (1999). Natural adjuvants: endogenous activators of dendritic cells. *Nat. Med.* 5, 1249–1255. doi: 10.1038/15200
- Grass, S., Lichti, C. F., Townsend, R. R., Gross, J., and St Geme, J. W. III. (2010). The *Haemophilus influenzae* HMW1C protein is a glycosyltransferase that transfers hexose residues to asparagine sites in the HMW1 adhesin. *PLoS Pathog.* 6:e1000919. doi: 10.1371/journal.ppat.1000919
- Hajishengallis, G. (2015). Periodontitis: from microbial immune subversion to systemic inflammation. *Nat. Rev. Immunol.* 15, 30–44. doi: 10.1038/nri3785
- Hajishengallis, G., and Lamont, R. J. (2012). Beyond the red complex and into more complexity: the polymicrobial synergy and dysbiosis (PSD) model of periodontal disease etiology. *Mol. Oral Microbiol.* 27, 409–419. doi: 10.1111/j.2041-1014.2012.00663.x
- Harding, C. M., Nasr, M. A., Kinsella, R. L., Scott, N. E., Foster, L. J., Weber, B. S., et al. (2015). Acinetobacter strains carry two functional oligosaccharyltransferases, one devoted exclusively to type IV pilin, and the

- other one dedicated to O-glycosylation of multiple proteins. *Mol. Microbiol.* 96, 1023–1041. doi: 10.1111/mmi.12986
- Hartley, M. D., Morrison, M. J., Aas, F. E., Borud, B., Koomey, M., and Imperiali, B. (2011). Biochemical characterization of the O-linked glycosylation pathway in *Neisseria gonorrhoeae* responsible for biosynthesis of protein glycans containing N,N'-diacetylglucosamine. *Biochemistry* 50, 4936–4948. doi: 10.1021/bi2003372
- Holt, S. C., and Ebersole, J. L. (2005). *Porphyromonas gingivalis*, *Treponema denticola*, and *Tannerella forsythia*: the "red complex", a prototype polybacterial pathogenic consortium in periodontitis. *Periodontology* 38, 72–122. doi: 10.1111/j.1600-0757.2005.00113.x
- Honma, K., Inagaki, S., Okuda, K., Kuramitsu, H. K., and Sharma, A. (2007). Role of a *Tannerella forsythia* exopolysaccharide synthesis operon in biofilm development. *Microb. Pathog.* 42, 156–166. doi: 10.1016/j.micpath.2007.01.003
- Iwakura, Y., and Ishigame, H. (2006). The IL-23/IL-17 axis in inflammation. *J. Clin. Invest.* 116, 1218–1222. doi: 10.1172/JCI28508
- Iwashkiw, J. A., Fentabil, M. A., Faridmoayer, A., Mills, D. C., Peppler, M., Czibener, C., et al. (2012). Exploiting the *Campylobacter jejuni* protein glycosylation system for glycoengineering vaccines and diagnostic tools directed against brucellosis. *Microb. Cell Fact.* 11:13. doi: 10.1186/1475-2859-11-13
- Iwashkiw, J. A., Voza, N. F., Kinsella, R. L., and Feldman, M. F. (2013). Pour some sugar on it: the expanding world of bacterial protein O-linked glycosylation. *Mol. Microbiol.* 89, 14–28. doi: 10.1111/mmi.12265
- Kassebaum, N. J., Bernabe, E., Dahiya, M., Bhandari, B., Murray, C. J., and Marcenes, W. (2014). Global burden of severe periodontitis in 1990–2010: a systematic review and meta-regression. *J. Dent. Res.* 93, 1045–1053. doi: 10.1177/0022034514552491
- Ku, S. C., Schulz, B. L., Power, P. M., and Jennings, M. P. (2009). The pilin O-glycosylation pathway of pathogenic *Neisseria* is a general system that glycosylates AniA, an outer membrane nitrite reductase. *Biochem. Biophys. Res. Commun.* 378, 84–89. doi: 10.1016/j.bbrc.2008.11.025
- Laemmli, U. K. (1970). Cleavage of structural proteins during the assembly of the head of bacteriophage T4. *Nature* 227, 680–685. doi: 10.1038/227680a0
- Lamont, R. J., and Hajishengallis, G. (2015). Polymicrobial synergy and dysbiosis in inflammatory disease. *Trends Mol. Med.* 21, 172–183. doi: 10.1016/j.molmed.2014.11.004
- Lanzinger, M., Jürgens, B., Hainz, U., Dillinger, B., Raberger, J., Fuchs, D., et al. (2012). Ambivalent effects of dendritic cells displaying prostaglandin E2-induced indoleamine 2,3-dioxygenase. *Eur. J. Immunol.* 42, 1117–1128. doi: 10.1002/eji.201141765
- Lebeer, S., Vanderleyden, J., and De Keersmaecker, S. C. (2010). Host interactions of probiotic bacterial surface molecules: comparison with commensals and pathogens. *Nat. Rev. Microbiol.* 8, 171–184. doi: 10.1038/nrmicro2297
- Lee, S. W., Sabet, M., Um, H. S., Yang, J., Kim, H. C., and Zhu, W. (2006). Identification and characterization of the genes encoding a unique surface (S-) layer of *Tannerella forsythia*. *Gene* 371, 102–111. doi: 10.1016/j.gene.2005.11.027
- Lees-Miller, R. G., Iwashkiw, J. A., Scott, N. E., Seper, A., Vinogradov, E., Schild, S., et al. (2013). A common pathway for O-linked protein-glycosylation and synthesis of capsule in *Acinetobacter baumannii*. *Mol. Microbiol.* 89, 816–830. doi: 10.1111/mmi.12300
- Lithgow, K. V., Scott, N. E., Iwashkiw, J. A., Thomson, E. L. S., Foster, L. J., Feldman, M. F., et al. (2014). A general protein O-glycosylation system within the *Burkholderia cepacia* complex is involved in motility and virulence. *Mol. Microbiol.* 92, 116–137. doi: 10.1111/mmi.12540
- Lutz, M. B., and Schuler, G. (2002). Immature, semi-mature and fully mature dendritic cells: which signals induce tolerance or immunity? *Trends Immunol.* 23, 445–449. doi: 10.1016/S1471-4906(02)02281-0
- Lyons, A. B., and Parish, C. R. (1994). Determination of lymphocyte division by flow cytometry. *J. Immunol. Methods* 171, 131–137. doi: 10.1016/0022-1759(94)90236-4
- Martin, J. L., and McMillan, F. M. (2002). SAM (dependent) I AM: the S-adenosylmethionine-dependent methyltransferase fold. *Curr. Opin. Struct. Biol.* 12, 783–793. doi: 10.1016/S0959-440X(02)00391-3
- Medema, M. H., Takano, E., and Breitling, R. (2013). Detecting sequence homology at the gene cluster level with MultiGeneBlast. *Mol. Biol. Evol.* 30, 1218–1223. doi: 10.1093/molbev/mst025
- Merad, M., Sathe, P., Helft, J., Miller, J., and Mortha, A. (2013). The dendritic cell lineage: ontogeny and function of dendritic cells and their subsets in the steady state and the inflamed setting. *Annu. Rev. Immunol.* 31, 563–604. doi: 10.1146/annurev-immunol-020711-074950
- Nothaft, H., and Szymanski, C. M. (2010). Protein glycosylation in bacteria: sweeter than ever. *Nat. Rev. Microbiol.* 8, 765–778. doi: 10.1038/nrmicro2383
- Oh, Y. J., Sekot, G., Duman, M., Chtcheglova, L., Messner, P., Peterlik, H., et al. (2013). Characterizing the S-layer structure and anti-S-layer antibody recognition on intact *Tannerella forsythia* cells by scanning probe microscopy and small angle X-ray scattering. *J. Mol. Recognit.* 26, 542–549. doi: 10.1002/jmr.2298
- Ohyama, H., Kato-Kogoe, N., Kuhara, A., Nishimura, F., Nakasho, K., Yamanegi, K., et al. (2009). The involvement of IL-23 and the Th17 pathway in periodontitis. *J. Dent. Res.* 88, 633–638. doi: 10.1177/0022034509339889
- Posch, G., Pabst, M., Brecker, L., Altmann, F., Messner, P., and Schäffer, C. (2011). Characterization and scope of S-layer protein O-glycosylation in *Tannerella forsythia*. *J. Biol. Chem.* 286, 38714–38724. doi: 10.1074/jbc.M111.284893
- Posch, G., Pabst, M., Neumann, L., Coyne, M. J., Altmann, F., Messner, P., et al. (2013). "Cross-glycosylation" of proteins in Bacteroidales species. *Glycobiology* 23, 568–577. doi: 10.1093/glycob/cws172
- Reis e Sousa, C. (2006). Dendritic cells in a mature age. *Nat. Rev. Immunol.* 6, 476–483. doi: 10.1038/nri1845
- Sabet, M., Lee, S. W., Nauman, R. K., Sims, T., and Um, H.-S. (2003). The surface (S-) layer is a virulence factor of *Bacteroides forsythus*. *Microbiology* 149, 3617–3627. doi: 10.1099/mic.0.26535-0
- Sakakibara, J., Nagano, K., Murakami, Y., Higuchi, N., Nakamura, H., Shimoza, K., et al. (2007). Loss of adherence ability to human gingival epithelial cells in S-layer protein-deficient mutants of *Tannerella forsythensis*. *Microbiology* 153, 866–876. doi: 10.1099/mic.0.29275-0
- Schäffer, C., and Messner, P. (2017). Emerging facets of prokaryotic glycosylation. *FEMS Microbiol. Rev.* 41, 49–91. doi: 10.1093/femsre/fuw036
- Schubert, H. L., Blumenthal, R. M., and Cheng, X. (2003). Many paths to methyltransferase: a chronicle of convergence. *Trends Biochem. Sci.* 28, 329–335. doi: 10.1016/S0968-0004(03)00090-2
- Schwarz, F., Fan, Y. Y., Schubert, M., and Aebi, M. (2011). Cytoplasmic N-glycosyltransferase of *Actinobacillus pleuropneumoniae* is an inverting enzyme and recognizes the NX(S/T) consensus sequence. *J. Biol. Chem.* 286, 35267–35274. doi: 10.1074/jbc.M111.277160
- Sekot, G., Posch, G., Messner, P., Matejka, M., Rausch-Fan, X., Andrukhov, O., et al. (2011). Potential of the *Tannerella forsythia* S-layer to delay the immune response. *J. Dent. Res.* 90, 109–114. doi: 10.1177/0022034510384622
- Sekot, G., Posch, G., Oh, Y. J., Zayni, S., Mayer, H. F., Pum, D., et al. (2012). Analysis of the cell surface layer ultrastructure of the oral pathogen *Tannerella forsythia*. *Arch. Microbiol.* 194, 525–539. doi: 10.1007/s00203-012-0792-3
- Settem, R. P., Honma, K., Nakajima, T., Phansopa, C., Roy, S., Stafford, G. P., et al. (2013). A bacterial glycan core linked to surface (S-) layer proteins modulates host immunity through Th17 suppression. *Mucosal Immunol.* 6, 415–426. doi: 10.1038/mi.2012.85
- Settem, R. P., Honma, K., and Sharma, A. (2014). Neutrophil mobilization by surface-glycan altered th17-skewing bacteria mitigates periodontal pathogen persistence and associated alveolar bone loss. *PLoS One* 9:e108030. doi: 10.1371/journal.pone.0108030
- Sharma, A. (2010). Virulence mechanisms of *Tannerella forsythia*. *Periodontol.* 2000, 106–116. doi: 10.1111/j.1600-0757.2009.00332.x
- Sharma, A., Inagaki, S., Honma, K., Sfintescu, C., Baker, P. J., and Evans, R. T. (2005). *Tannerella forsythia*-induced alveolar bone loss in mice involves leucine-rich-repeat BspA protein. *J. Dent. Res.* 84, 462–467. doi: 10.1177/154405910508400512
- Socransky, S., Haffajee, A., Cugini, M., Smith, C., and Kent, R. (1998). Microbial complexes in subgingival plaque. *J. Clin. Periodontol.* 25, 134–144. doi: 10.1111/j.1600-051X.1998.tb02419.x
- Stafford, G. P., Chaudhuri, R. R., Haraszthy, V., Friedrich, V., Schäffer, C., Ruscitto, A., et al. (2016). Draft genome sequences of three clinical isolates of *Tannerella forsythia* isolated from subgingival plaque from periodontitis patients in the United States. *Genome Announc.* 4:e01286-16. doi: 10.1128/genomeA.01286-16
- Staudacher, E. (2012). Methylation – an uncommon modification of glycans. *Biol. Chem.* 393, 675–685. doi: 10.1515/hsz-2012-0132



- Sutton, C. E., Lalor, S. J., Sweeney, C. M., Brereton, C. F., Lavelle, E. C., and Mills, K. H. (2009). Interleukin-1 and IL-23 induce innate IL-17 production from gammadelta T cells, amplifying Th17 responses and autoimmunity. *Immunity* 31, 331–341. doi: 10.1016/j.immuni.2009.08.001
- Szymanski, C. M., Logan, S. M., Linton, D., and Wren, B. W. (2003). *Campylobacter* – a tale of two protein glycosylation systems. *Trends Microbiol.* 11, 233–238. doi: 10.1016/S0966-842X(03)00079-9
- Szymanski, C. M., and Wren, B. W. (2005). Protein glycosylation in bacterial mucosal pathogens. *Nat. Rev. Microbiol.* 3, 225–237. doi: 10.1038/nrmicro1100
- Szymanski, C. M., Yao, R., Ewing, C. P., Trust, T. J., and Guerry, P. (1999). Evidence for a system of general protein glycosylation in *Campylobacter jejuni*. *Mol. Microbiol.* 32, 1022–1030. doi: 10.1046/j.1365-2958.1999.01415.x
- Tanner, A., Listgarten, M., Ebersole, J., and Strzempko, M. (1986). *Bacteroides forsythus* sp. nov., a slow-growing, fusiform *Bacteroides* sp. from the human oral cavity. *Int. J. Syst. Evol. Microbiol.* 36, 213–221. doi: 10.1099/00207713-36-2-213
- Tomek, M. B., Janesch, B., Maresch, D., Windwarder, M., Altmann, F., Messner, P., et al. (2017). A pseudaminic acid or a legionaminic acid derivative transferase is strain-specifically implicated in the general protein O-glycosylation system of the periodontal pathogen *Tannerella forsythia*. *Glycobiology* 27, 555–567. doi: 10.1093/glycob/cwx019
- Tomek, M. B., Neumann, L., Nimeth, I., Koerd, A., Andesner, P., Messner, P., et al. (2014). The S-layer proteins of *Tannerella forsythia* are secreted via a type IX secretion system that is decoupled from protein O-glycosylation. *Mol. Oral Microbiol.* 29, 307–320. doi: 10.1111/omi.12062
- Upreti, R. K., Kumar, M., and Shankar, V. (2003). Bacterial glycoproteins: functions, biosynthesis and applications. *Proteomics* 3, 363–379. doi: 10.1002/pmic.200390052
- Valguarnera, E., Kinsella, R. L., and Feldman, M. F. (2016). Sugar and spice make bacteria not nice: protein glycosylation and its influence in pathogenesis. *J. Mol. Biol.* 428, 3206–3220. doi: 10.1016/j.jmb.2016.04.013
- Varki, A., Cummings, R. D., Aebi, M., Packer, N. H., Seeberger, P. H., Esko, J. D., et al. (2015). Symbol nomenclature for graphical representations of glycans. *Glycobiology* 25, 1323–1324. doi: 10.1093/glycob/cwv091
- Varki, A., Cummings, R. D., Esko, J. D., Stanley, P., and Hart, G. W. (2017). *Essentials of Glycobiology*. Cold Spring, NY: Cold Spring Harbor Laboratory Press.
- Vartoukian, S. R. (2016). Cultivation strategies for growth of uncultivated bacteria. *J. Oral Biosci.* 58, 142–149. doi: 10.1016/j.job.2016.08.001
- Vik, Å., Aas, F. E., Anonsen, J. H., Bilsborough, S., Schneider, A., Egge-Jacobsen, W., et al. (2009). Broad spectrum O-linked protein glycosylation in the human pathogen *Neisseria gonorrhoeae*. *Proc. Natl. Acad. Sci. U.S.A.* 106, 4447–4452. doi: 10.1073/pnas.0809504106
- Wohlschlager, T., Butschli, A., Grassi, P., Sutov, G., Gauss, R., Hauck, D., et al. (2014). Methylated glycans as conserved targets of animal and fungal innate defense. *Proc. Natl. Acad. Sci. U.S.A.* 111, E2787–E2796. doi: 10.1073/pnas.1401176111
- Yoneda, M., Hirofujii, T., Motooka, N., Nozoe, K., Shigenaga, K., Anan, H., et al. (2003). Humoral immune responses to S-layer-like proteins of *Bacteroides forsythus*. *Clin. Diagn. Lab. Immunol.* 10, 383–387. doi: 10.1128/CDLI.10.3.383-387.2003
- Zarschler, K., Janesch, B., Zayni, S., Schäffer, C., and Messner, P. (2009). Construction of a gene knockout system for application in *Paenibacillus alvei* CCM 2051T, exemplified by the S-layer glycan biosynthesis initiation enzyme WsfP. *Appl. Environ. Microbiol.* 75, 3077–3085. doi: 10.1128/AEM.00087-09

**Conflict of Interest Statement:** The authors declare that the research was conducted in the absence of any commercial or financial relationships that could be construed as a potential conflict of interest.

Copyright © 2018 Tomek, Maresch, Windwarder, Friedrich, Janesch, Fuchs, Neumann, Nimeth, Zwickl, Dohm, Everest-Dass, Kolarich, Himmelbauer, Altmann and Schäffer. This is an open-access article distributed under the terms of the Creative Commons Attribution License (CC BY). The use, distribution or reproduction in other forums is permitted, provided the original author(s) and the copyright owner(s) are credited and that the original publication in this journal is cited, in accordance with accepted academic practice. No use, distribution or reproduction is permitted which does not comply with these terms.